

# Supporting information

## Tuning the Dual Inhibition of Carbonic Anhydrase and Cyclooxygenase by Dihydrothiazole Benzensulfonamides

Rita Meleddu, Simona Distinto, Filippo Cottiglia, Rossella Angius, Marco Gaspari, Domenico Taverna, Claudia Melis, Andrea Angeli, Giulia Bianco, Serenella Deplano, Benedetta Fois, Sonia Del Prete, Clemente Capasso, Stefano Alcaro, Francesco Ortuso, Matilde Yanez, Claudiu T. Supuran and Elias Maccioni.

### Sommario

Chemistry .....	2
General methods.....	2
Synthesis and characterization.....	2
Table S1: Experimental data of compound EMAC10110 and compounds EMAC10111 a-g .....	5
Table S2: calculated and experimental mass values for EMAC 10111 a-g and blank full scan spectra. ....	6
Mass spectra of compounds EMAC 10111 a-g (Figures S1-S8).....	6
<sup>1</sup> H NMR of compounds EMAC10111 a-g (Figures S9-S15) .....	11
<sup>13</sup> C NMR of compounds EMAC10111 a-g (Figures S16-S22) .....	14
Molecular modelling .....	18
Biological evaluation.....	25
Carbonic anhydrase inhibition assay .....	25
Determination of human cyclooxygenase isoform activity .....	25
References .....	26

## Chemistry

### General methods

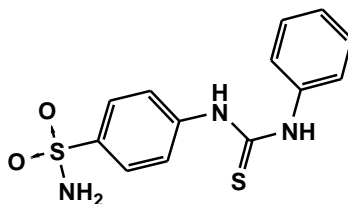
Reagents and solvents were obtained from commercial suppliers and were used without further purification. All melting points were determined by the capillary method on a Stuart SMP30 Digital Advanced apparatus and are uncorrected.

Mass spectra were registered on a Q-Exactive mass spectrometer (Thermo Fisher Scientific, Germany). Compounds were initially dissolved in dimethylsulfoxide (DMSO) at 1 mg/mL concentration. Stock solutions were then diluted 100-fold in ethanol:water 4:1 containing 0.1% of formic acid. Mass spectra were acquired on a Q-Exactive mass spectrometer (Thermo Fisher Scientific) via a nano-electrospray interface operating in positive ion mode. Ion transfer tube temperature was 250 °C, whereas S-lens value was 50 units. Full MS spectra were acquired at resolution of 140,000, in the m/z range 200-800, using an in-source CID of 20 eV in order to minimize the presence of adducts with DMSO. Mass spectra are reported in Figures S2-S8. <sup>1</sup>H-NMR and <sup>13</sup>C-NMR chemical shifts of compounds EMAC are reported and spectra are depicted in Figures S9-S22. All samples were measured in DMSO-d<sub>6</sub> at 278.1 K temperature on a Bruker 400 MHz or on a Varian 500 MHz spectrometer. Chemical shifts are reported in ppm. Coupling constants J are expressed in hertz (Hz).

TLC chromatography was performed using silica gel plates (Merck F254), spots were visualized by UV light.

### Synthesis and characterization

#### Synthesis of 1-phenyl-3-(4-sulfamoylphenyl)thiourea (EMAC10110)



4-amidobenzensulphonamide (1 eq.) was refluxed in 2-propanol until a clear solution is obtained. Then a solution of phenyl-isothiocyanate (1 eq.) in 2-propanol was added dropwise. By adding the isothiocyanate the solution became yellowish. The mixture was stirred until reaction completion (5-6 h) monitored by TLC (ethyl acetate/n-hexane 2/1). The reaction is allowed to cool down at r.t. and the formation of a white foaming precipitate is observed, which was filtered and crystallized from ethanol.

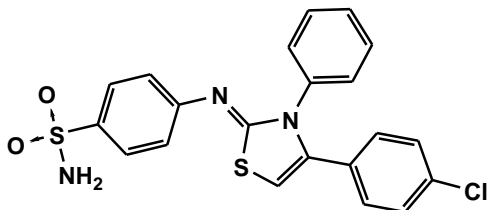
White crystals; MW: 307.39 g/mol; yield: 50%; Mp: 195-197 °C

<sup>1</sup>H-NMR: (500 MHz, DMSO); 10.01 (bs, 2H, NH), 7.75 (d, 2H, J: 10, -CH, Ar.), 7.68 (d, 2H, J: 10, -CH Ar), 7.15 (t, 2H, J: 10, -CH Ar), 7.48 (d, 2H, J: 10, -CH Ar), 7.34 (t, 1H, J: 10, -CH Ar), 7.26 (s, 2H, -NH).

#### General method for the synthesis of 4-aryl-3-phenylthiazol-2(3H)-ylideneamino)benzenesulfonamides EMAC10111 a-g

1-phenyl-3-(4-sulfamoylphenyl)thiourea (1 eq) was suspended in 2-propanol and the appropriate alpha haloketone (1 eq) was added. Then the mixture was heated ad 50°C until a solution is formed. The reaction was monitored by TLC (ethyl acetate/n-hexane 2/1) and heating prolonged for a time ranging from 3 to 7 hours until a foamy precipitate is formed. By cooling to rt an abundant precipitate is formed which was filtered and crystallized from the appropriate solvent.

**4-(4-(4-chlorophenyl)-3-phenylthiazol-2(3H)-ylideneamino)benzenesulfonamide (EMAC10111a)**

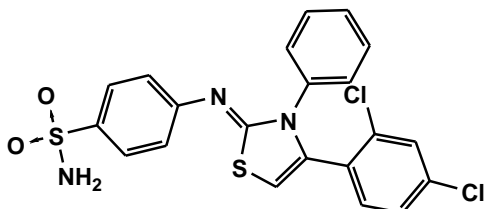


MW: 441.95 g/mol; yield: 53%

<sup>1</sup>H-NMR (400 MHz, DMSO)  $\delta$ : 7.86 (d, 2H, J: 9, -CH Ar), 7.47- 7.46 (m, 4H), 7.37- 7.34 (m, 5H), 7.19 (d, 2H, J: 9, -CH Ar), 6.99 (s, 1H, thiaz.), 5.58 (brs, 2H, NH<sub>2</sub>).

<sup>13</sup>C NMR (101 MHz, DMSO)  $\delta$  157.70 (1C), 152.98 (1C), 138.82 (1C), 137.31 (1C), 137.25 (1C), 134.08 (1C), 131.98 (1C), 130.55 (1C), 129.51 (1C), 129.13 (1C), 128.99 (1C), 128.88 (2C), 128.41 (1C), 128.37 (2C), 127.96 (1C), 127.58 (1C), 127.57 (2C), 85.69 (1C).

**4-(4-(2,4-dichlorophenyl)-3-phenylthiazol-2(3H)-ylideneamino) benzenesulfonamide (EMAC10111b)**

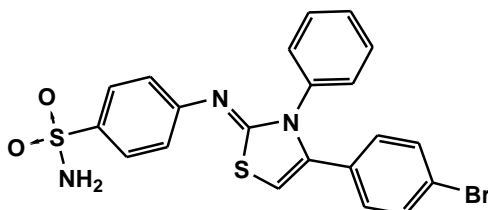


MW: 476.4 g/mol; yield: 47%

<sup>1</sup>H-NMR: (400 MHz, DMSO)  $\delta$ : 7.75 (d, 2H, J: 9, -CH Ar), 7.57-7.54 (m [dd+s], 2H, -CH Ar, 2-4Cl), 7.41 (dd, 1H, J<sub>o</sub>: 8.4, J<sub>m</sub>: 8.4, -CH Ar), 7.36-7.23 (m, 7H, -CH Ar+ NH<sub>2</sub>), 7.09 (d, 2H J: 9, -CH Ar), 6.59 (s, 1H, thiaz).

<sup>13</sup>C NMR: (101 MHz, DMSO)  $\delta$  159.28 (1C), 154.05 (1C), 138.06 (1C), 136.59 (1C), 134.88 (1C), 134.79 (1C), 134.24 (1C), 134.14 (1C), 129.10 (1C), 128.81 (1C), 128.74 (2C), 128.67 (2C), 128.09 (1C), 127.45 (2C), 127.27 (1C), 121.06 (2C), 99.76 (1C).

**4-(4-(4-bromophenyl)-3-phenylthiazol-2(3H)-ylideneamino)benzene sulfonamide (EMAC10111c)**

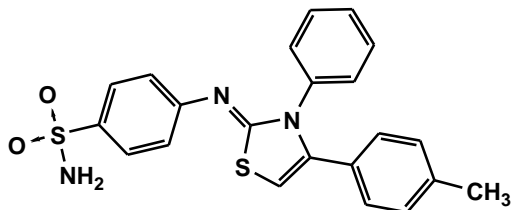


MW: 486.4 g/mol; yield: 60%

<sup>1</sup>H-NMR: (400 MHz, DMSO)  $\delta$ : 7.76 (d, 2H, J: 8.4, -CH Ar), 7.50-7.43 (m, 7H), 7.38-7.39 (m, 2H), 7.12 (d, 2H, J: 8.8, -CH Ar), 7.00 (s, 1H, thiazole), 5.79 (bs, 2H, -NH<sub>2</sub>).

<sup>13</sup>C NMR (101 MHz, DMSO)  $\delta$  157.66 (1C), 153.01 (1C), 138.82 (1C), 137.35 (1C), 137.25 (1C), 132.18 (1C), 131.33 (1C), 131.29 (2C), 130.72 (1C), 129.49 (1C), 129.12 (1C), 129.00 (1C), 128.88 (1C), 128.36 (1C), 128.33 (1C), 127.58 (2C), 122.83 (1C), 121.06 (1C), 85.64 (1C).

**4-(4-(4-methylphenyl)-3-phenylthiazol-2(3H)-ylideneamino)benzene sulfonamide (EMAC10111d)**

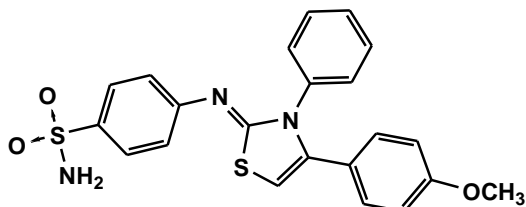


MW: 421.54 g/mol; yield: 68%

<sup>1</sup>H-NMR: (400 MHz, DMSO)  $\delta$ : 7.88 (d, 2H, J: 8.4, -CH Ar), 7.49-7.48 (m, 4H), 7.45-7.43 (m, 3H), 7.09-7.04 (m, 4H), 6.97 (m, 1H), 5.17 (bs, 2H, -NH<sub>2</sub>), 2.23 (s, 3H, -CH<sub>3</sub>).

<sup>13</sup>C NMR (101 MHz, DMSO)  $\delta$  157.94 (1C), 152.77 (1C), 140.76 (1C), 138.58 (1C), 137.42 (1C), 129.92 (1C), 129.60 (1C), 129.12 (1C), 128.92 (1C), 128.86 (4C), 128.73 (1C), 127.57 (2C), 126.65 (1C), 126.05 (1C), 123.06 (1C), 121.15 (1C), 84.95 (1C), 25.45 (1C).

**4-(4-(4-methoxyphenyl)-3-phenylthiazol-2(3H)-ylideneamino)benzene sulfonamide (EMAC10111e)**

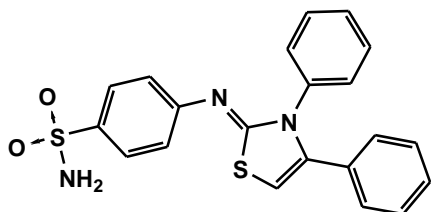


MW: 437.5 g/mol; yield: 69%

<sup>1</sup>H-NMR: (400 MHz, DMSO)  $\delta$ : 7.84(d, 2H, J: 8.4, -CH Ar), 7.46-7.45 (m, 4H), 7.36-7.32 (m, 4H), 7.09 (d, 2H, J: 8.8), 6.82 (d, 2H, J: 8.8), 4.13 (brs, 2H, -NH<sub>2</sub>), 3.70 (s, 3H, -OCH<sub>3</sub>).

<sup>13</sup>C NMR (101 MHz, DMSO)  $\delta$  159.48 (1C), 157.75 (1C), 153.22 (1C), 138.63 (1C), 138.41 (1C), 137.56 (1C), 131.51 (1C), 130.08 (1C), 129.31 (1C), 129.15 (1C), 128.95 (1C), 128.89 (1C), 127.55 (1C), 127.50 (2C), 121.07 (2C), 120.99 (1C), 113.68 (2C), 84.48 (1C), 55.12 (1C).

**4-(3,4-diphenylthiazol-2(3H)-ylideneamino)benzenesulfonamide (EMAC10111f)**

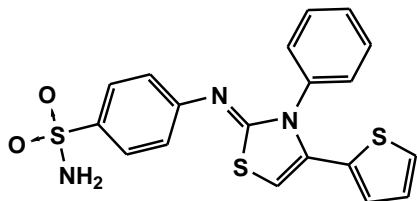


MW: 407.5 g/mol; yield: 38%

<sup>1</sup>H-NMR: (400 MHz, DMSO)  $\delta$ : 7.74 (d, 2H, J: 8.8, -CH Ar), 7.39-7.35 (m, 2H), 7.31-7.28 (m, 3H), 7.25-7.22 (m, 5H), 7.17-7.15 (m, 2H), 7.04 (d, 2H, J: 8.8, -CH Ar), 6.54 (s, 1H, thiazole).

<sup>13</sup>C NMR (101 MHz, DMSO)  $\delta$  160.19 (1C), 154.22 (1C), 139.29 (1C), 137.98 (1C), 137.56 (1C), 130.86 (1C), 129.02 (2C), 128.86 (2C), 128.48 (1C), 128.26 (2C), 128.21 (2C), 127.85 (1C), 127.42 (2C), 121.12 (2C), 97.93 (1C).

**4-(4-(4-thiophenophenyl)-3-phenylthiazol-2(3H)-ylideneamino)benzene sulfonamide (EMAC10111g)**



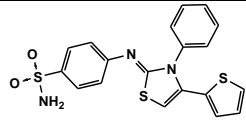
MW: 413.5 g/mol; yield: 44%

<sup>1</sup>H-NMR: (400 MHz, DMSO)  $\delta$ : 7.74 (d, 2H, J: 8.4, -CH Ar), 7.49-7.47 (m, 2H), 7.46-7.42 (m, 2H), 7.39-7.37 (m, 2H), 7.22 (m, 2H), 7.06 (d, 2H, J: 8.4), 6.83 (t, 1H, J: 3.6, J: 1.2) 6.84 (dd, 1H, J: 3.6, J: 1.2), 6.70 (s, 1H thiazole).

<sup>13</sup>C NMR (101 MHz, DMSO)  $\delta$  160.87 (1C), 164.07 (1C), 138.06 (1C), 137.22 (1C), 132.83 (1C), 131.39 (1C), 129.57 (2C), 129.24 (2C), 128.77 (1C), 127.79 (1C), 127.74 (1C), 127.41 (2C), 127.06 (1C), 121.10 (2C), 98.03 (1C).

**Table S1: Experimental data of compound EMAC10110 and compounds EMAC10111 a-g**

Compound	R.F.*	Molecular Formula	CHN calc.	M.P. °C	Crist solv.	colour
			CHN found			
 EMAC10110	0.54	C <sub>13</sub> H <sub>13</sub> N <sub>3</sub> O <sub>2</sub> S <sub>2</sub>	C, 50.79; H, 4.26; N, 13.67 C, 51.95; H, 4.30; N, 14.02	195-197	ethanol	white solid
 EMAC10111a	0.67	C <sub>21</sub> H <sub>16</sub> ClN <sub>3</sub> O <sub>2</sub> S <sub>2</sub>	C, 57.07; H, 3.65; N, 9.51 C, 56.79; H, 4.05; N, 10.01	241.7 - 242.7	ethanol	white solid
 EMAC10111b	0.64	C <sub>21</sub> H <sub>15</sub> Cl <sub>2</sub> N <sub>3</sub> O <sub>2</sub> S <sub>2</sub>	C, 52.94; H, 3.17; N, 8.82 C, 54.02; H, 2.99; N, 8.60	251.6 -252	acetonitrile/ethanol	white crystals
 EMAC10111c	0.65	C <sub>21</sub> H <sub>16</sub> BrN <sub>3</sub> O <sub>2</sub> S <sub>2</sub>	C, 51.85; H, 3.32; N, 8.64 C, 53.02; H, 3.28; N, 8.37	243-244	ethanol	white crystals
 EMAC10111d	0.66	C <sub>22</sub> H <sub>19</sub> N <sub>3</sub> O <sub>2</sub> S <sub>2</sub>	C, 62.68; H, 4.54; N, 9.97 C, 63.14; H, 4.38; N, 9.66	175.5 -176	ethanol	white crystals
 EMAC10111e	0.58	C <sub>22</sub> H <sub>19</sub> N <sub>3</sub> O <sub>3</sub> S <sub>2</sub>	C, 60.39; H, 4.38; N, 9.60 C, 61.11; H, 4.40; N, 9.90	238-239	ethanol	white crystals
 EMAC10111f	0.64	C <sub>21</sub> H <sub>17</sub> N <sub>3</sub> O <sub>2</sub> S <sub>2</sub>	C, 61.89; H, 4.20; N, 10.31 C, 63.37; H, 3.99; N, 10.71	292-292.5	ethanol	white crystals

 EMAC10111g	0.63	C <sub>19</sub> H <sub>15</sub> N <sub>3</sub> O <sub>2</sub> S <sub>3</sub>	C, 55.18; H, 3.66; N, 10.16	>280 d	ethanol	Pale yellow crystals
			C, 55.73; H, 3.40; N, 9.97			

\*R.F.ethyl acetate/n-exane 2/1

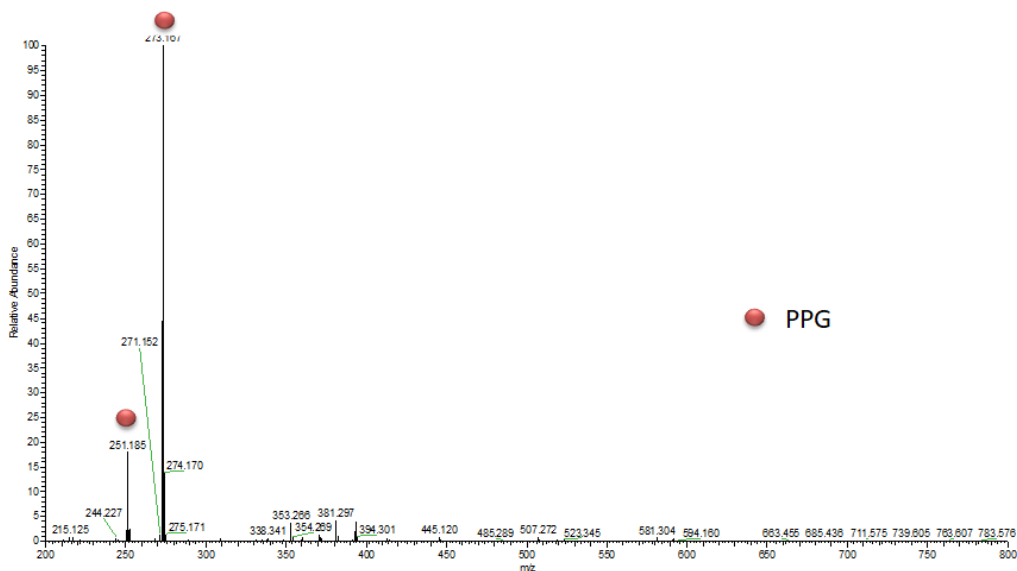
**Table S2: calculated and experimental mass values for EMAC 10111 a-g and blank full scan spectra.**

Compound	Molecular Formula	Calculated[M+H] <sup>+</sup>	m/z, [M+H] <sup>+</sup>	delta m/z (ppm)
EMAC10111a	C <sub>21</sub> H <sub>16</sub> ClN <sub>3</sub> O <sub>2</sub> S <sub>2</sub>	442.0451	442.0448	-0.7
EMAC10111b	C <sub>21</sub> H <sub>15</sub> Cl <sub>2</sub> N <sub>3</sub> O <sub>2</sub> S <sub>2</sub>	476.0056	476.0058	0.4
EMAC10111c	C <sub>21</sub> H <sub>16</sub> BrN <sub>3</sub> O <sub>2</sub> S <sub>2</sub>	485.9946	485.9948	0.4
EMAC10111d	C <sub>22</sub> H <sub>19</sub> N <sub>3</sub> O <sub>2</sub> S <sub>2</sub>	422.0997	422.0990	-1.7
EMAC10111e	C <sub>22</sub> H <sub>19</sub> N <sub>3</sub> O <sub>3</sub> S <sub>2</sub>	438.0946	438.0936	-2.3
EMAC10111f	C <sub>21</sub> H <sub>17</sub> N <sub>3</sub> O <sub>2</sub> S <sub>2</sub>	408.084	408.0831	2.2
EMAC10111g	C <sub>19</sub> H <sub>15</sub> N <sub>3</sub> O <sub>2</sub> S <sub>3</sub>	414.0405	414.0396	-2.2

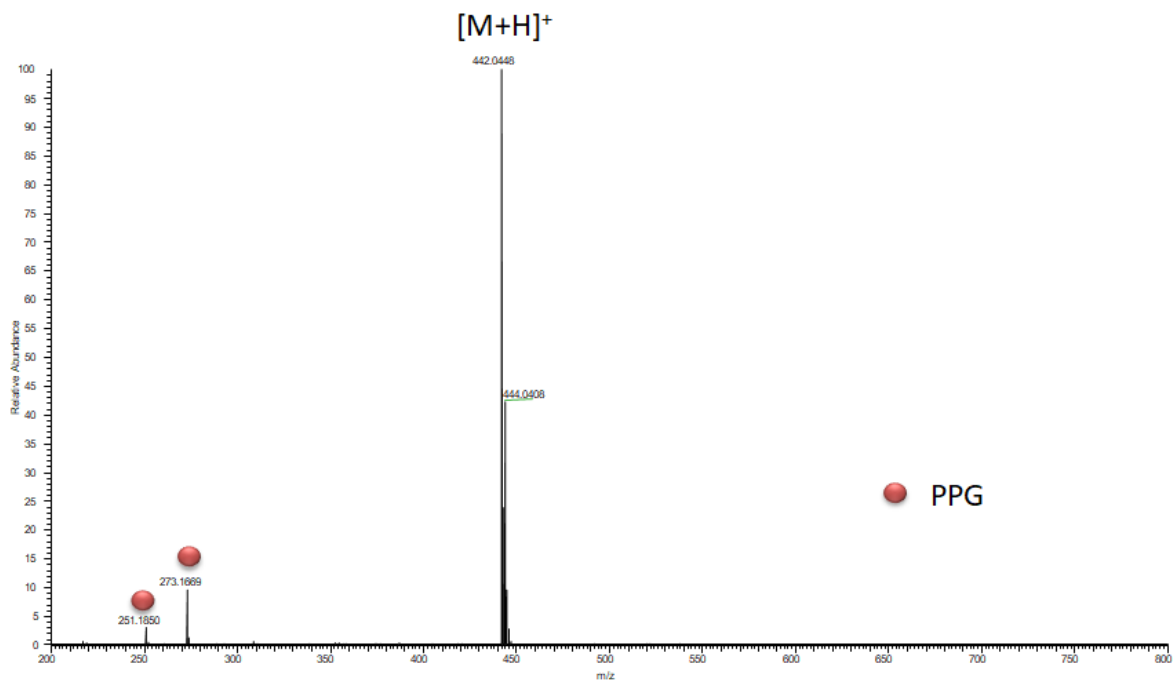
### Mass spectra of compounds EMAC 10111 a-g (Figures S1-S8)

#### S1: Full scan Mass Spectrum of blank solution (ethanol:water 4:1, 0,1% formic acid)

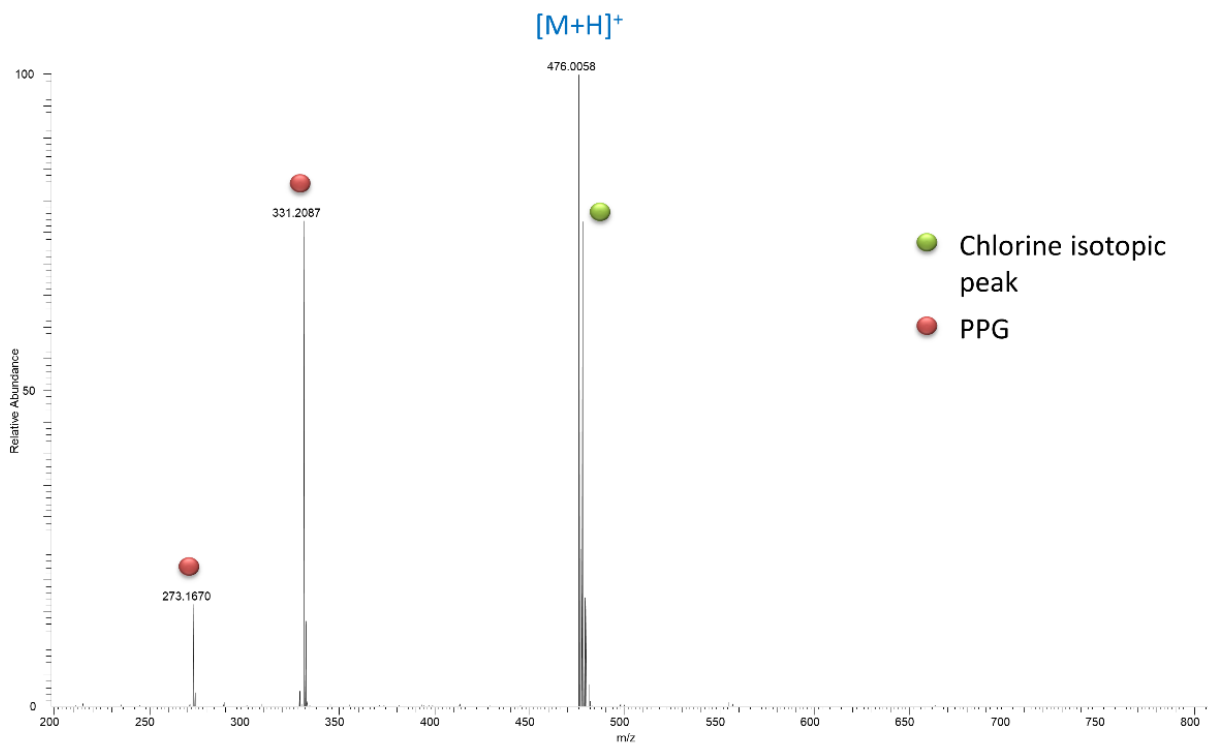
Blank  
full scan, 200-800 m/z  
positive polarity  
res power 140,000



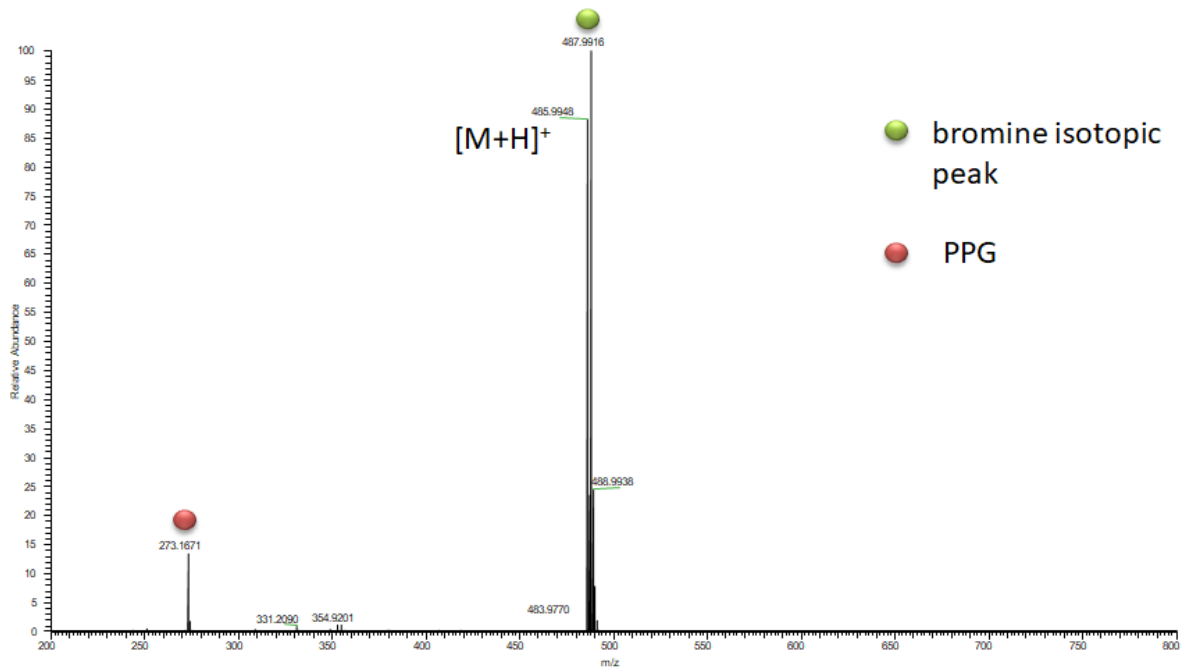
### S2: Full Mass Spectrum of compound EMAC10111a



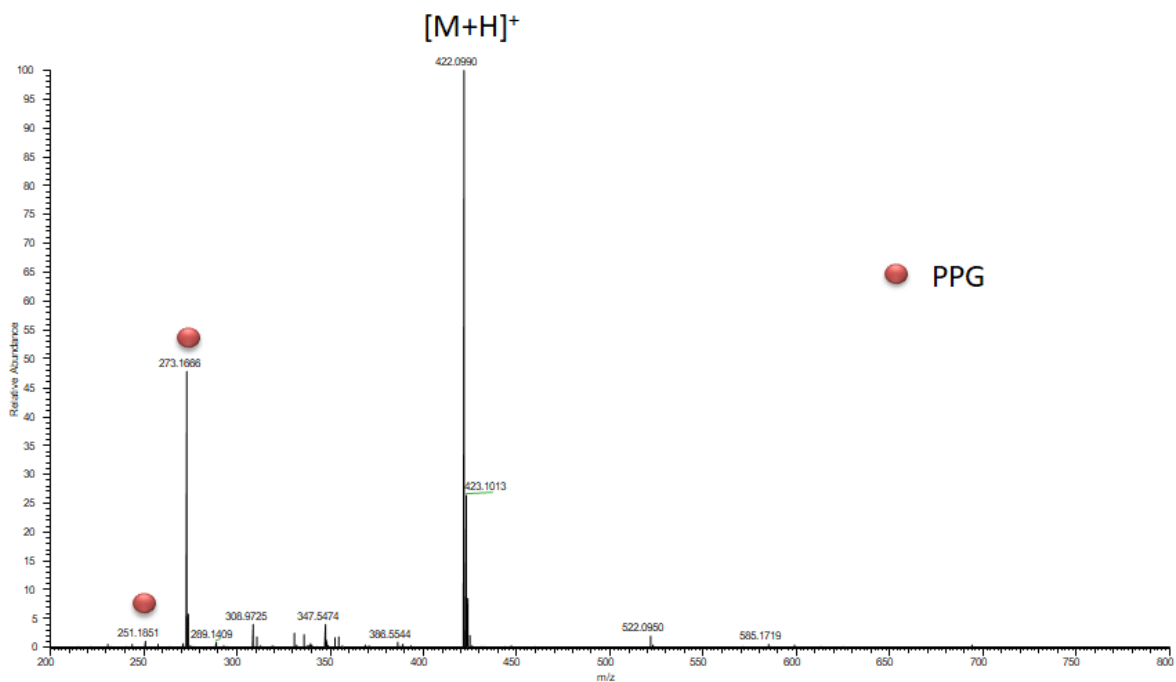
### S3: Full Mass Spectrum of compound EMAC10111b



#### S4: Full Mass Spectrum of compound EMAC10111c

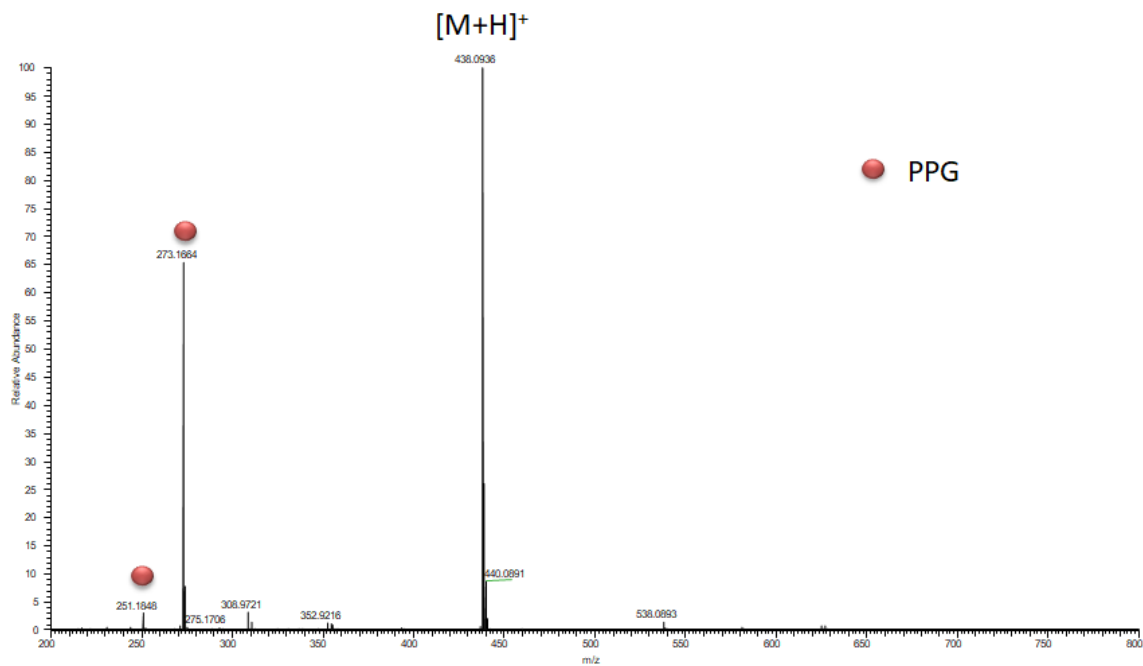


#### S5: Full Mass Spectrum of compound EMAC10111d

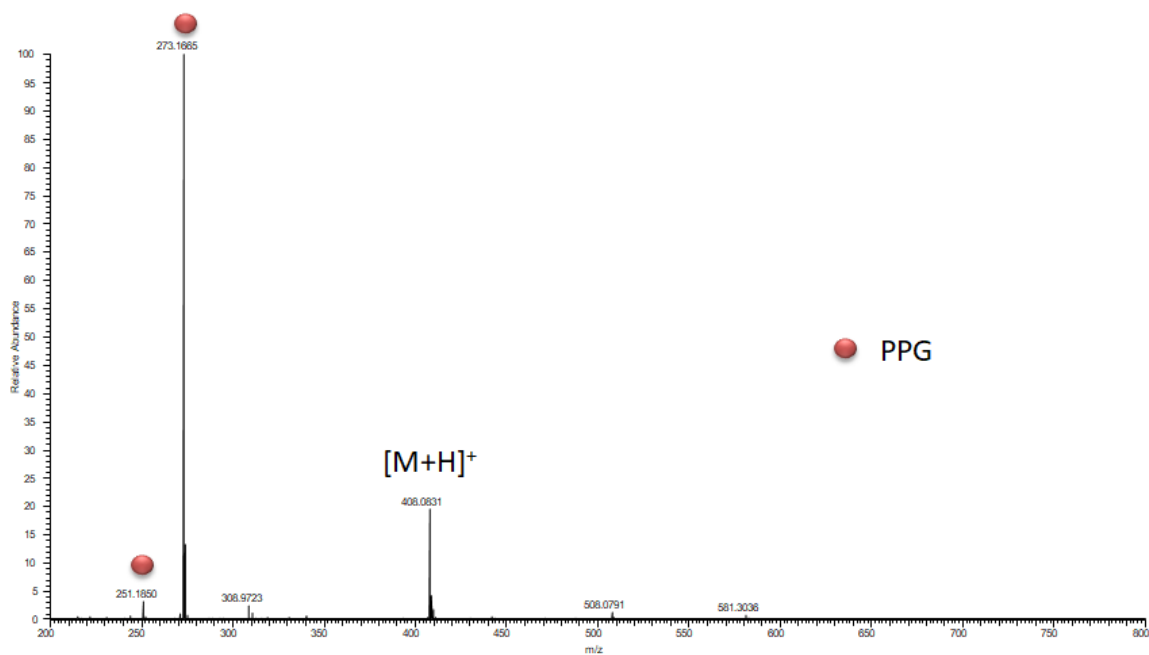




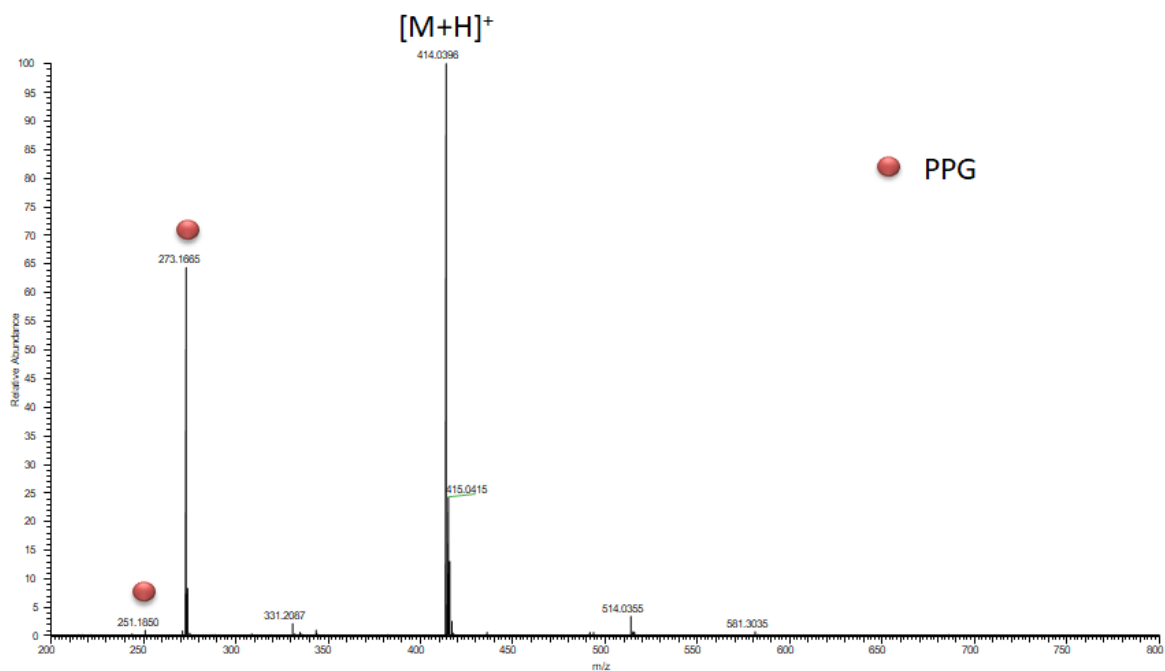
### S6: Full Mass Spectrum of compound EMAC10111e



### S7: Full Mass Spectrum of compound EMAC10111f

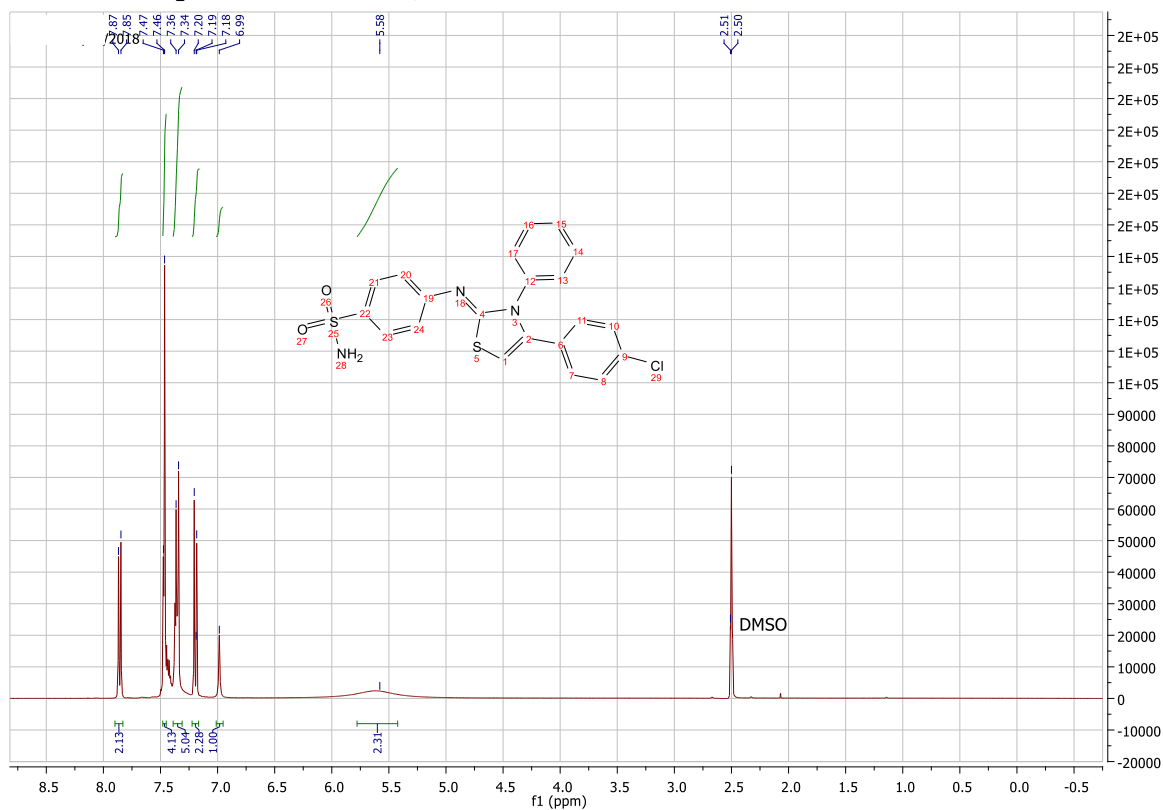


### S8: Full Mass Spectrum of compound EMAC1011g

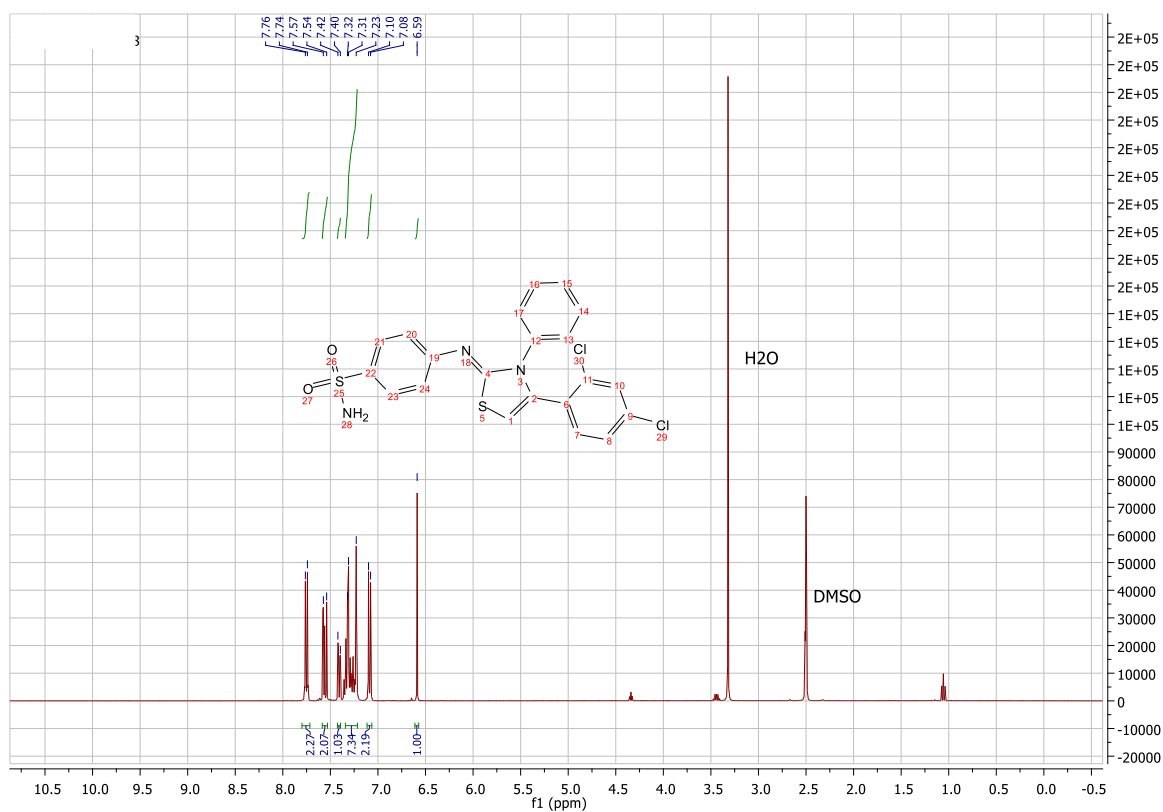


# <sup>1</sup>H NMR of compounds EMAC10111 a-g (Figures S9-S15)

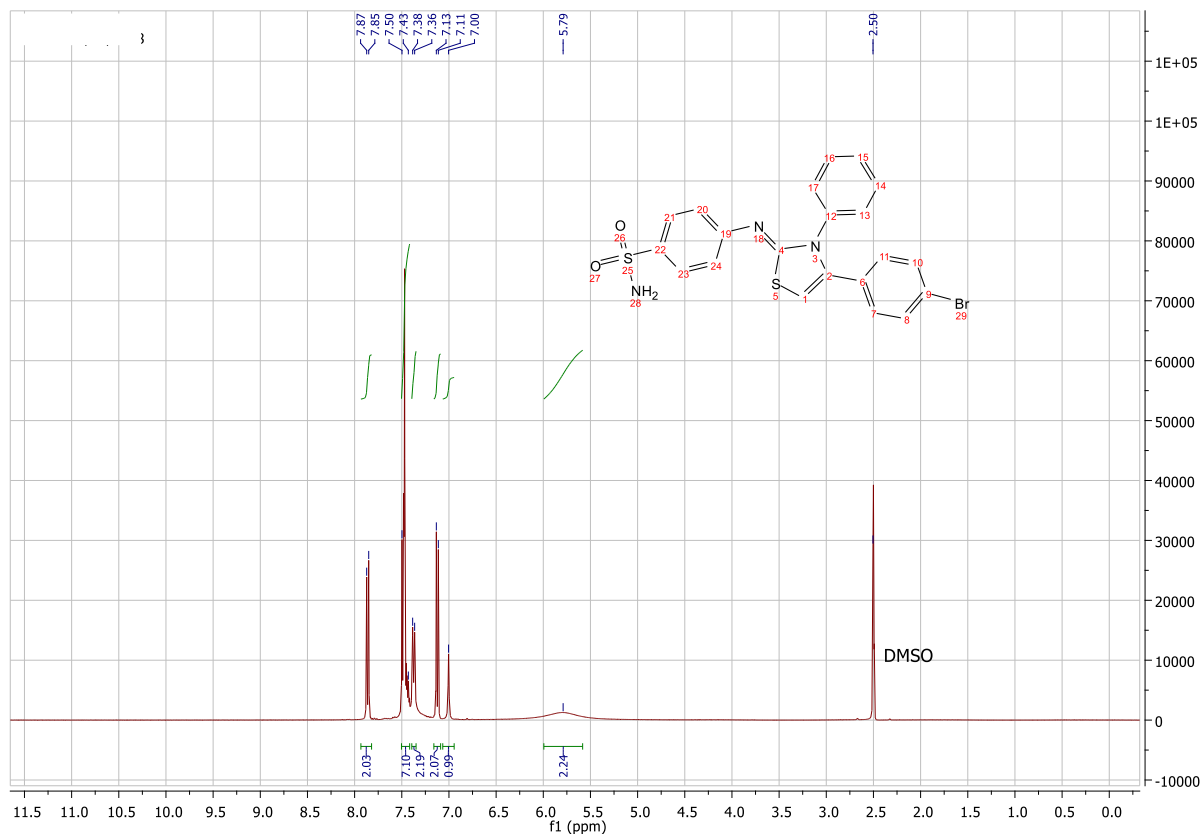
## S9: <sup>1</sup>H NMR spectrum (400 MHz, DMSO-d6) of EMAC10111a



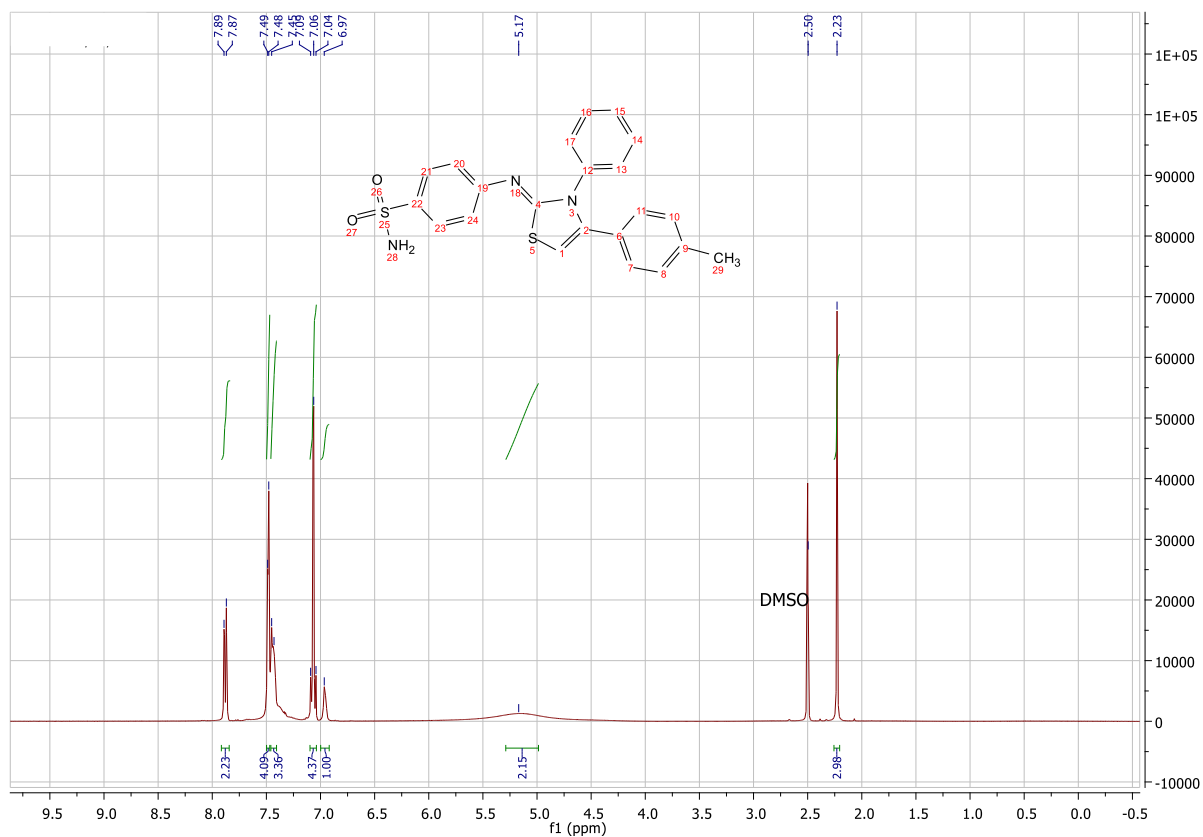
## S10: <sup>1</sup>H NMR spectrum (400 MHz, DMSO-d6) of EMAC10111b



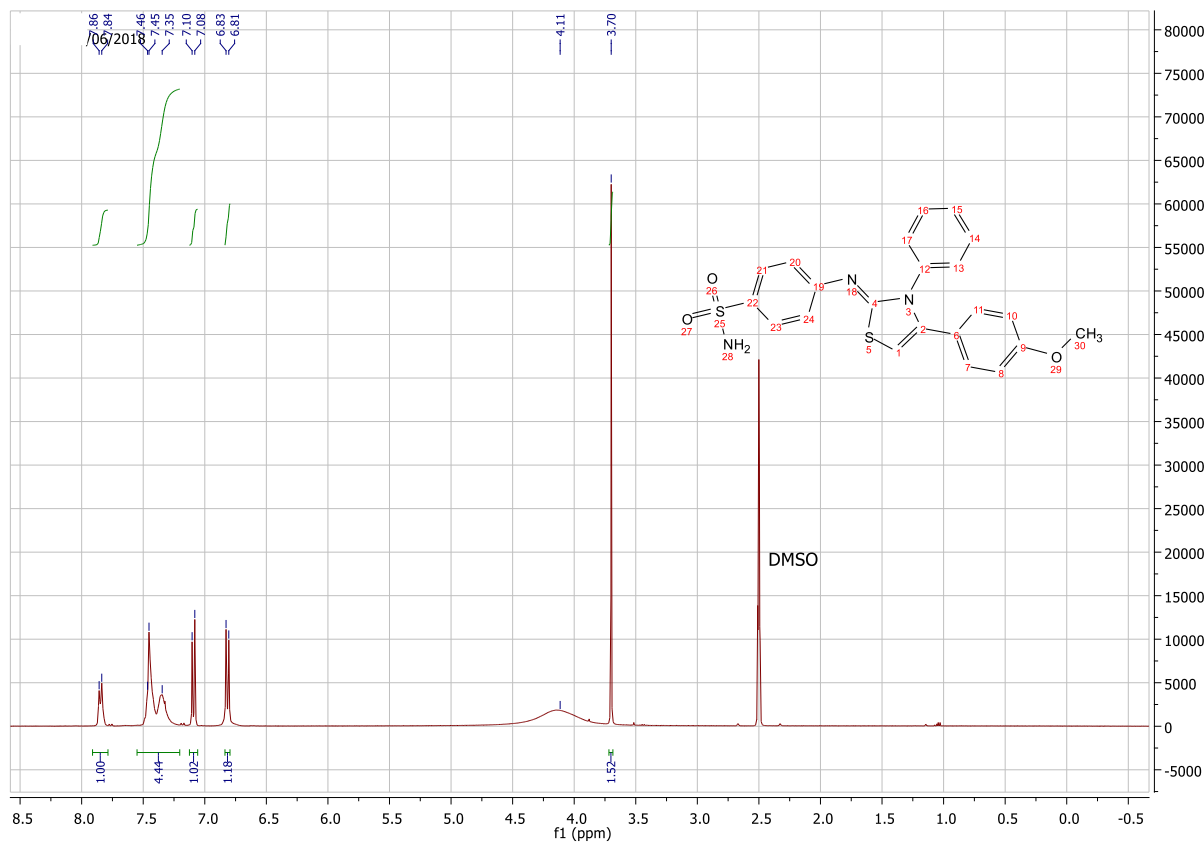
S11: <sup>1</sup>H NMR spectrum (400 MHz, DMSO-d<sub>6</sub>) of EMAC10111c



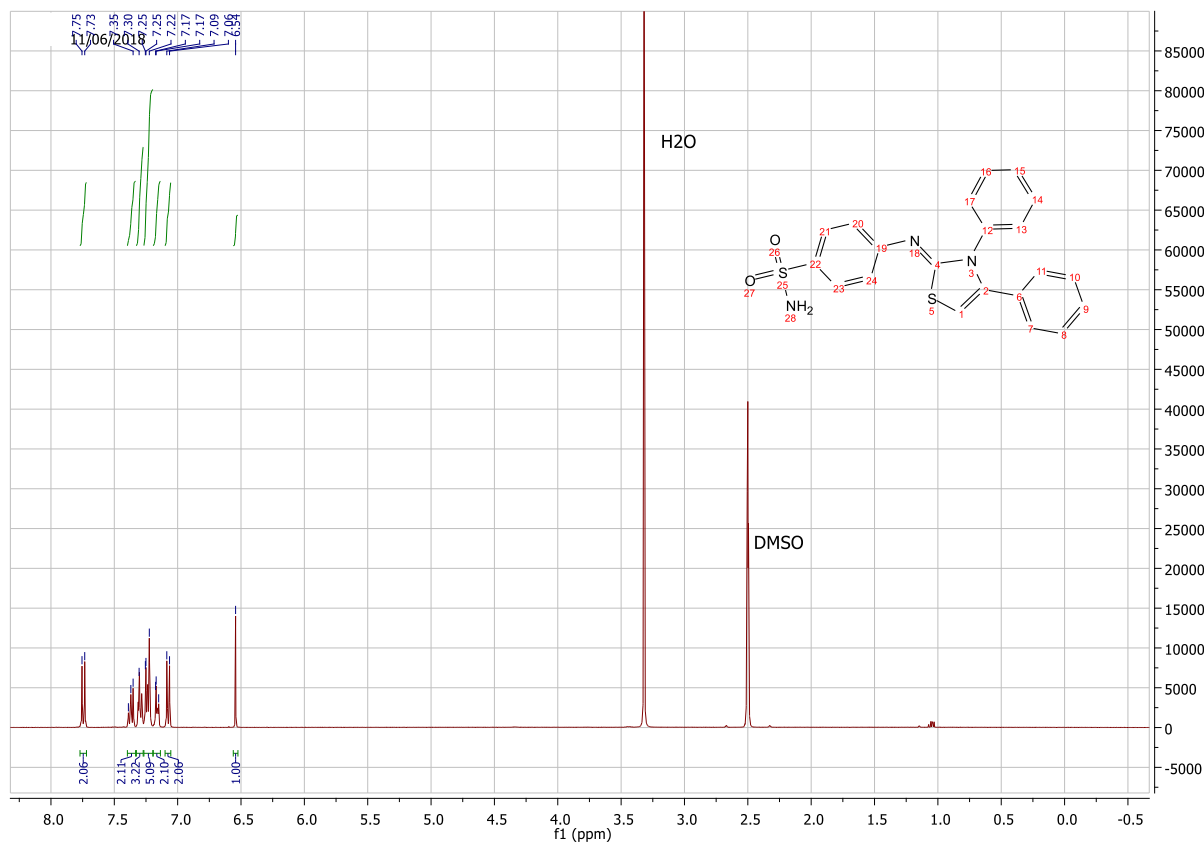
S12: <sup>1</sup>H NMR spectrum (400 MHz, DMSO-d<sub>6</sub>) of EMAC10111d



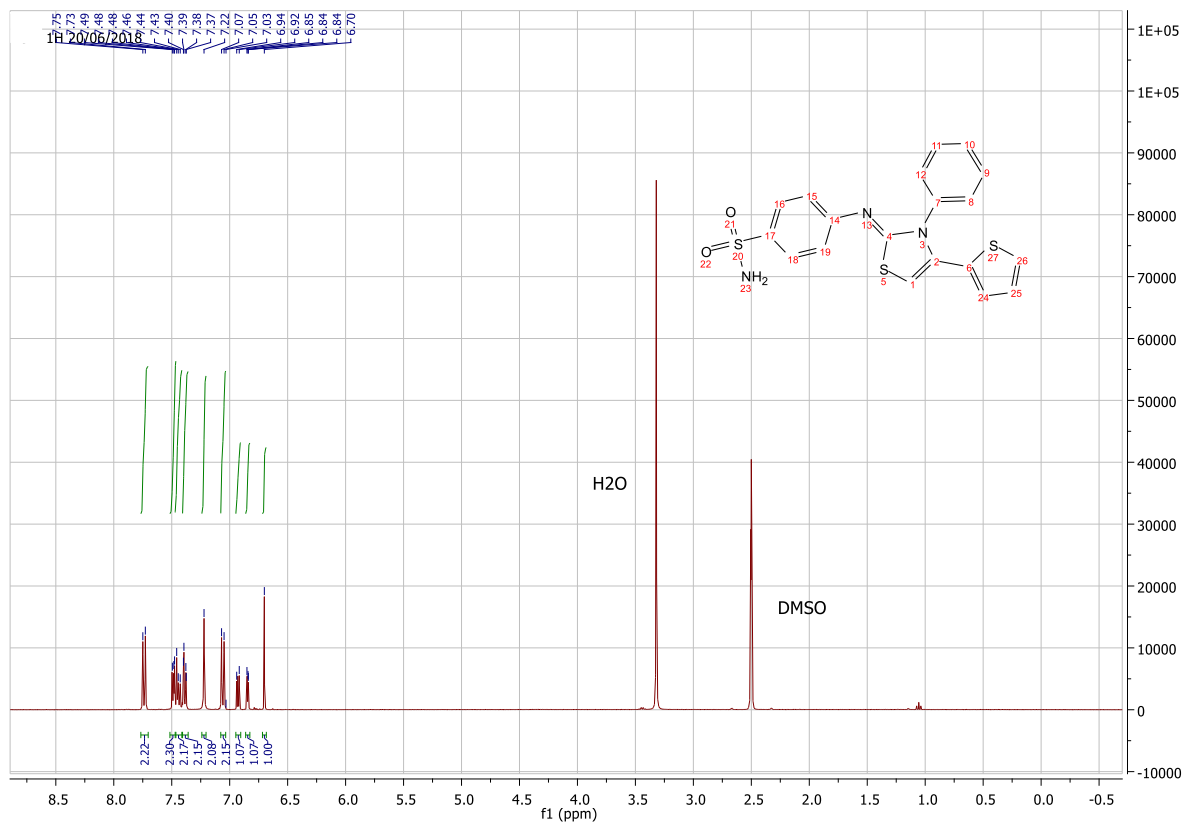
### S13: <sup>1</sup>H NMR spectrum (400 MHz, DMSO-d<sub>6</sub>) of EMAC10111e



### S14: <sup>1</sup>H NMR spectrum (400 MHz, DMSO-d<sub>6</sub>) of EMAC10111f

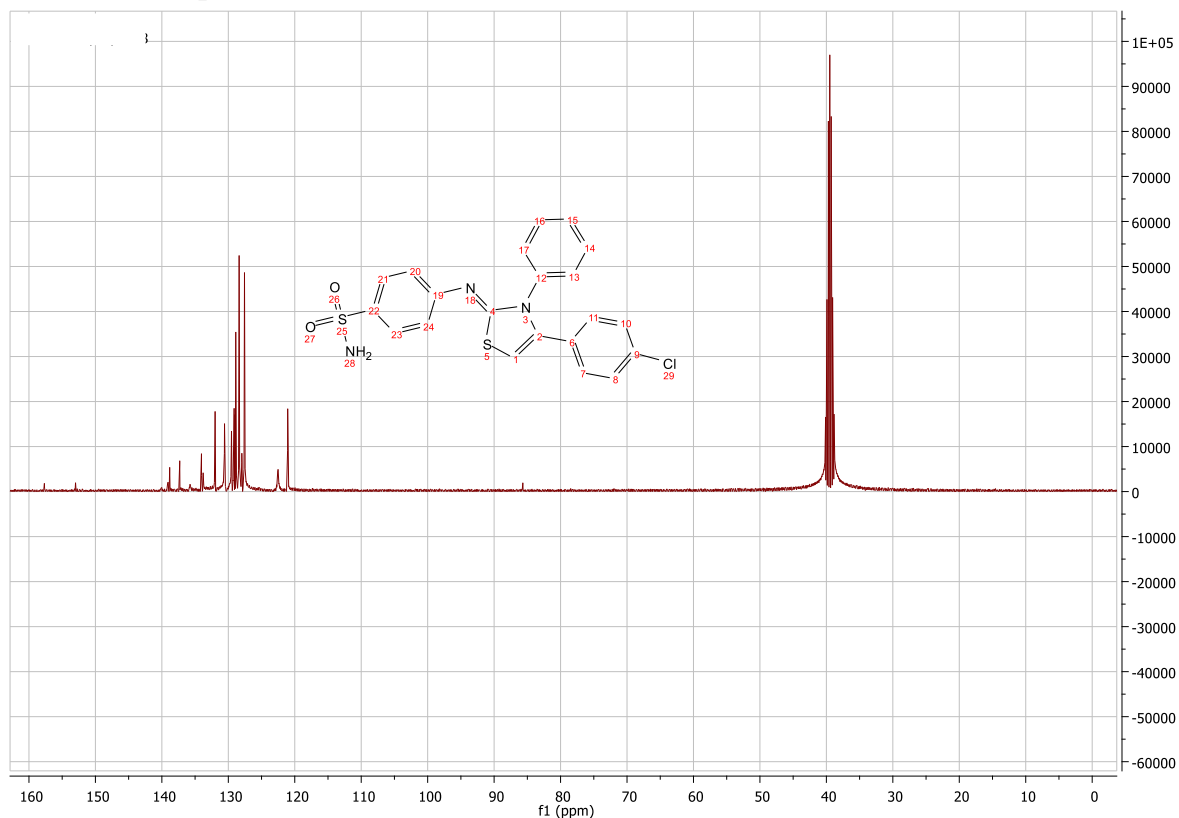


**S15: <sup>1</sup>H NMR spectrum (400 MHz, DMSO-d<sub>6</sub>) of EMAC10111g**

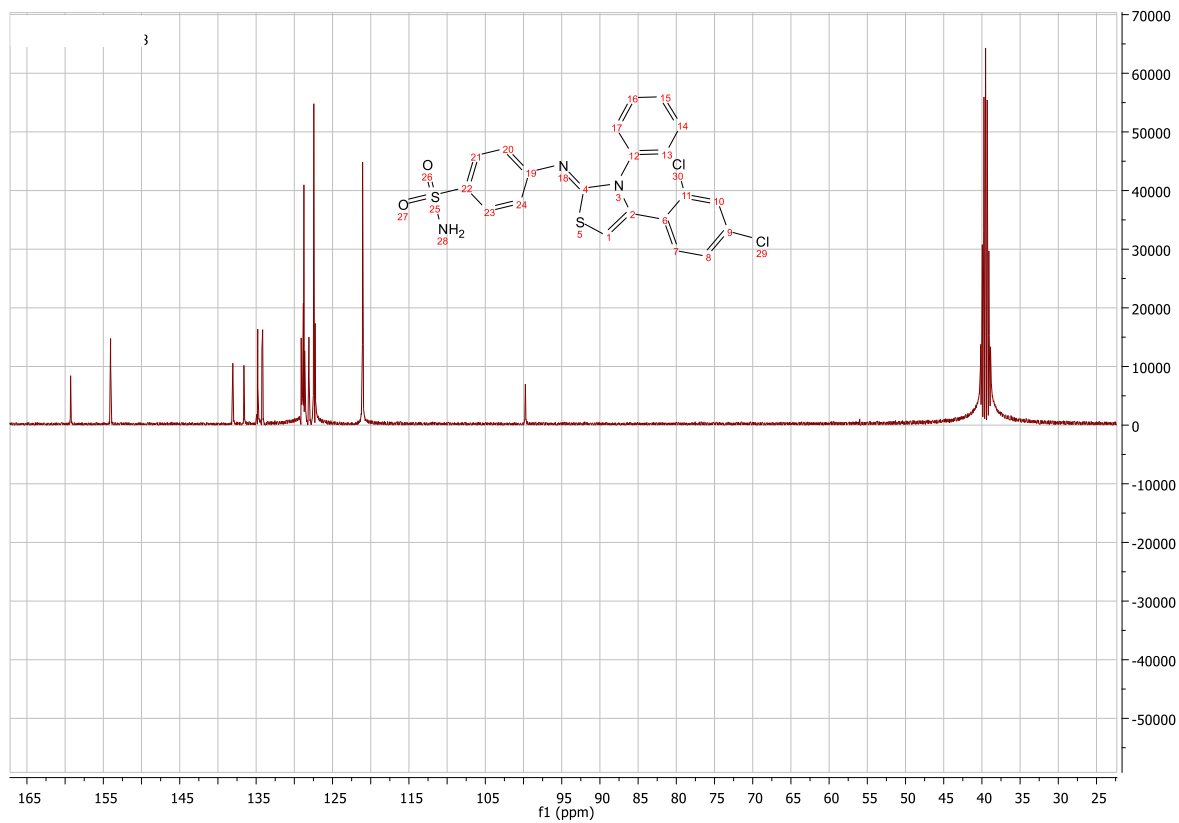


**<sup>13</sup>C NMR of compounds EMAC10111 a-g (Figures S16-S22)**

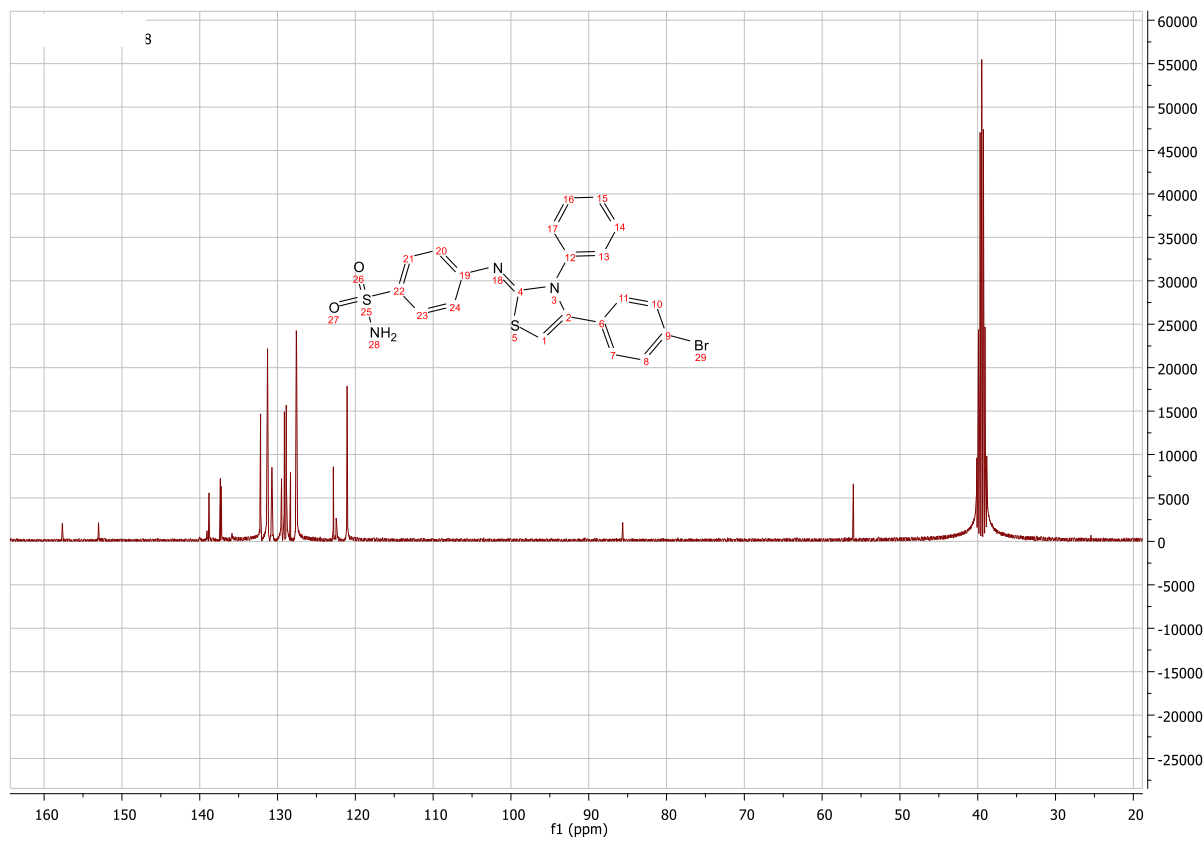
**S16: <sup>13</sup>C NMR spectrum (101 MHz, DMSO-d<sub>6</sub>) of EMAC10111a**



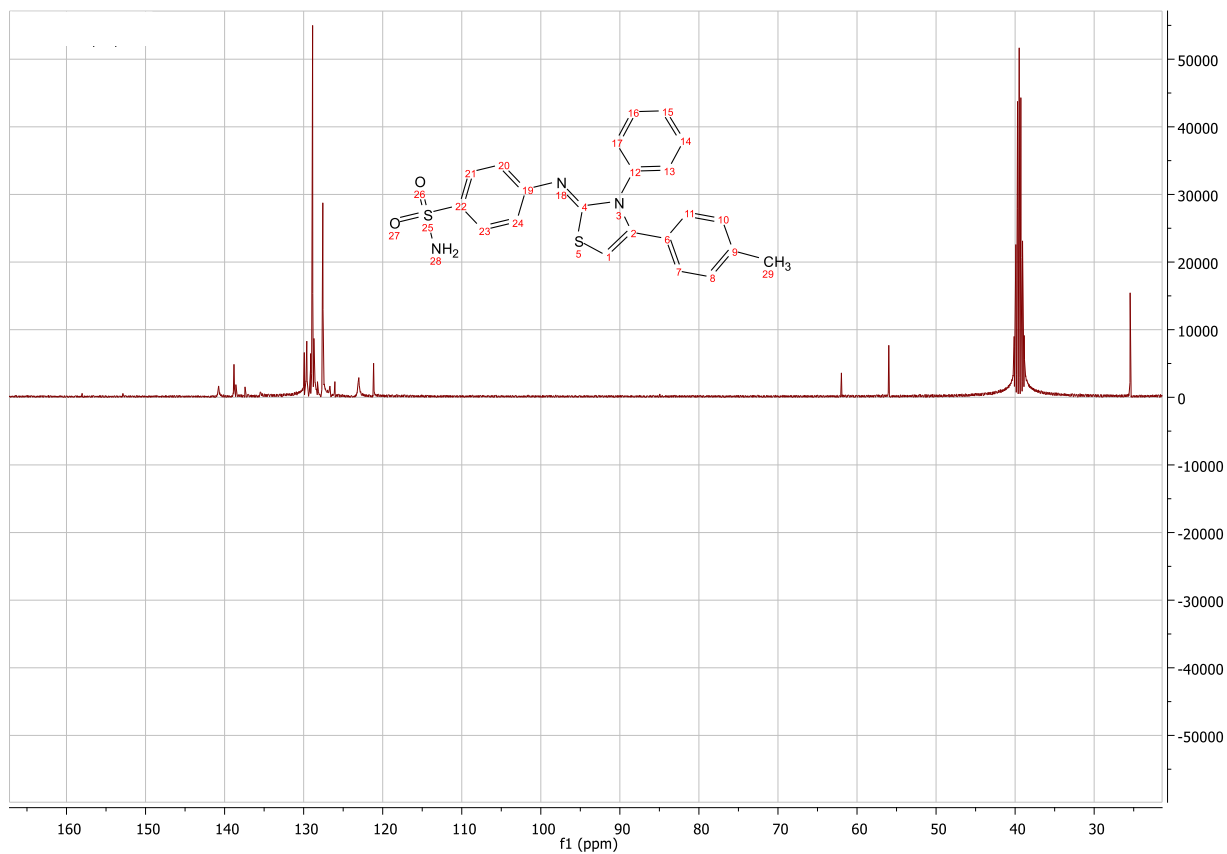
S17:  $^{13}\text{C}$  NMR spectrum (101 MHz, DMSO-d<sub>6</sub>) of EMAC10111b



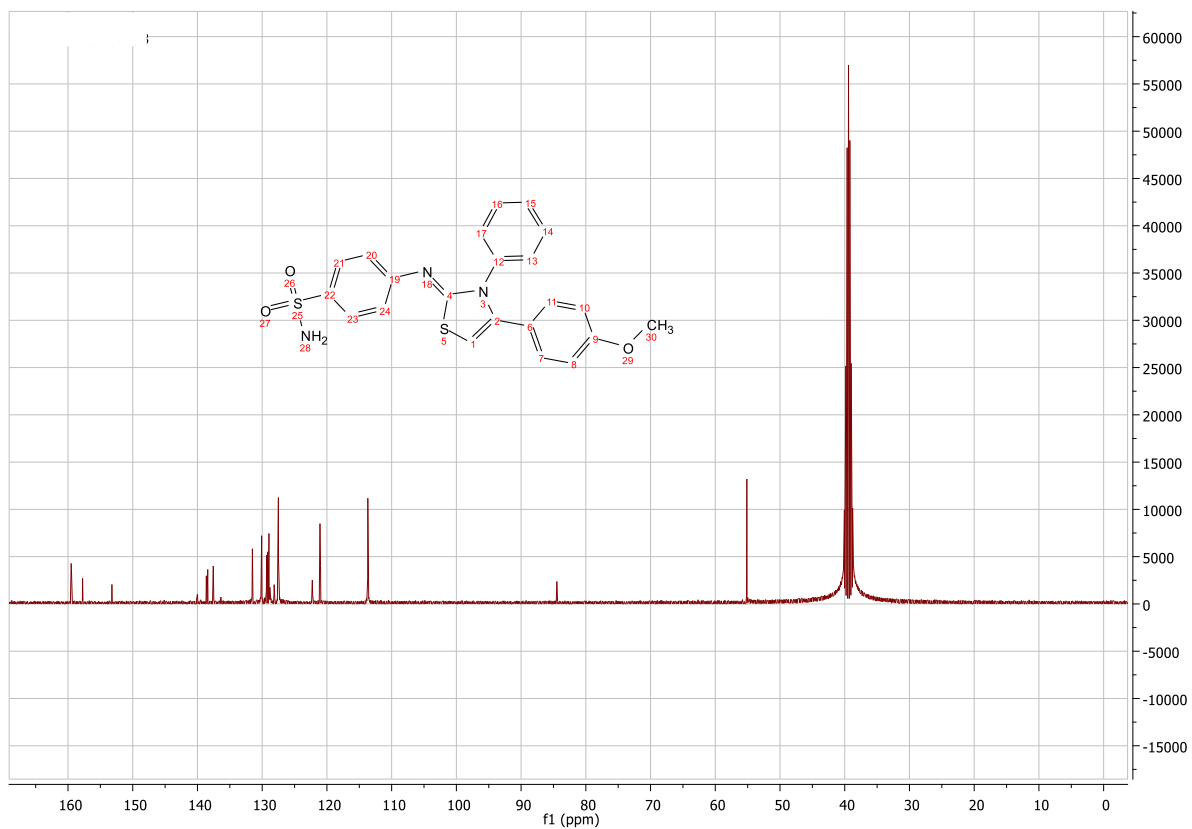
S18:  $^{13}\text{C}$  NMR spectrum (101 MHz, DMSO-d<sub>6</sub>) of EMAC10111c



S19:  $^{13}\text{C}$  NMR spectrum (101 MHz, DMSO-d<sub>6</sub>) of EMAC10111d

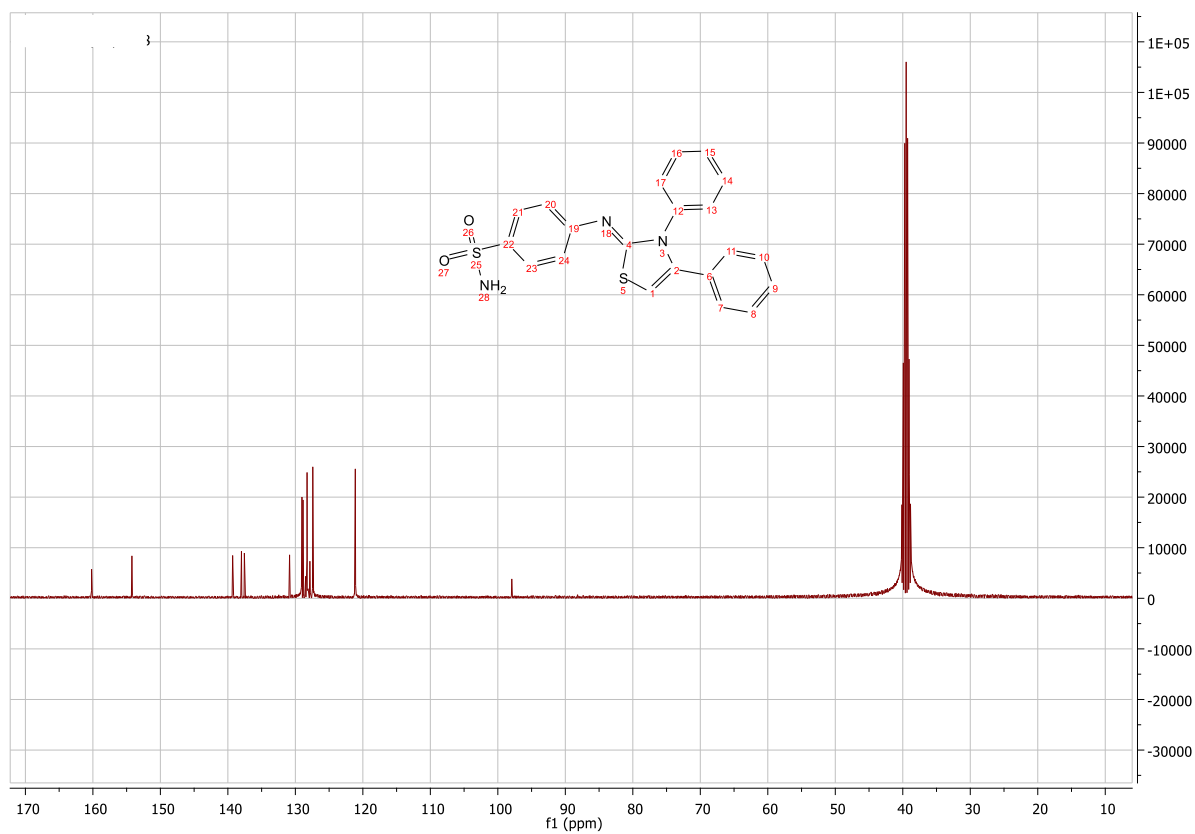


S20:  $^{13}\text{C}$  NMR spectrum (101 MHz, DMSO-d<sub>6</sub>) of EMAC10111e

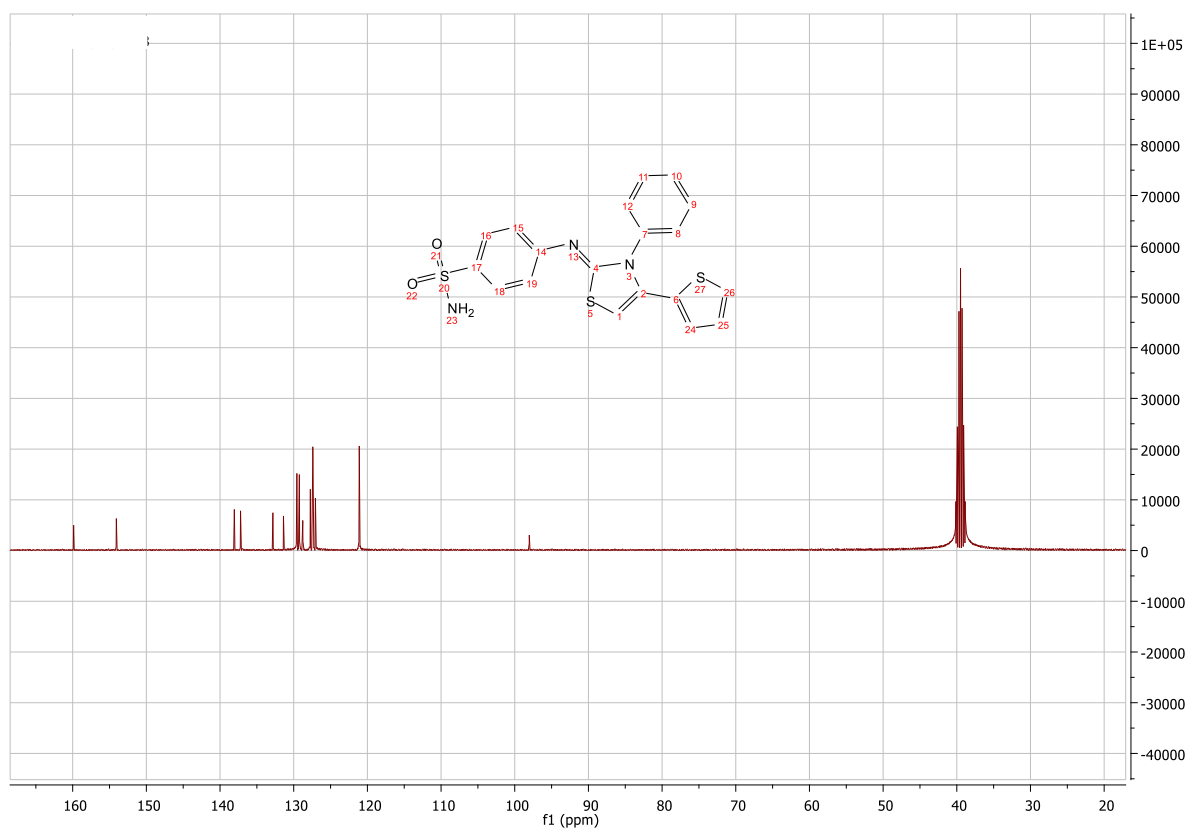




S21:  $^{13}\text{C}$  NMR spectrum (101 MHz, DMSO-d<sub>6</sub>) of EMAC10111f



S22:  $^{13}\text{C}$  NMR spectrum (101 MHz, DMSO-d<sub>6</sub>) of EMAC10111g



## **Molecular modelling**

### **Self and Cross Docking Ligands Preparation**

Theoretical 3D models of compounds downloaded from the PDB.<sup>1</sup> Ligands were protonated at physiological pH by means of LigPrep protocol<sup>2</sup> and docked in the global minimum energy conformation as determined by molecular mechanics conformational analysis performed with Macromodel software version 9.2.<sup>3</sup> All parameters were left as default. The geometry was optimized by MMFFs (Merck molecular force fields)<sup>4</sup> and GB/SA water implicit solvation model<sup>5</sup> using Polak-Ribier Conjugate Gradient (PRCG) method, 5000 iterations and a convergence criterion of 0.05 kcal/(mol Å).

### **Docking experiments on Human Cyclooxygenase 1 and 2**

#### **hCOX-2 protein preparation of**

Many Mus Musculus COX-2 complexes crystal structures are available in the PDB. Recently, some crystal structures of human COX-2 have been uploaded. The sequence and 3D alignment revealed a high percentage of identity as it can be observed in Figure S23 and 24.

6COX: A   PDBID   CHAIN   SEQUENCE	-----ANPCCSNPCQNRGECMSTGFDQYKDCDTRTGFYGENCTTPEFL	43
sp   P35354   PGH2_HUMAN	MLARALLCAVLALSHTANPCCSHPCQNRGVCMSVGFQYKDCDTRTGFYGENCSTPEFL	60
5F19: A   PDBID   CHAIN   SEQUENCE	-----KNPCCSHPCQNRGVCMSVGFQYKDCDTRTGFYGENCSTPEFL	43
	*****.***** ** .*****.*****.*****	
6COX: A   PDBID   CHAIN   SEQUENCE	TRIKLLLKPTPNTVHYILTHFKGFWNVVNNIPFLRSLIMKYVLTSRSLIDSPPTYNVHY	103
sp   P35354   PGH2_HUMAN	TRIKLFLKPTPNTVHYILTHFKGFWNVVNNIPFLRNAIMSYVLTSRSHLIDSPPTYNADY	120
5F19: A   PDBID   CHAIN   SEQUENCE	TRIKLFLKPTPNTVHYILTHFKGFWNVVNNIPFLRNAIMSYVLTSRSHLIDSPPTYNADY	103
	*****.*****.*****.*****.*****.*****.*****	
6COX: A   PDBID   CHAIN   SEQUENCE	GYKSWEAFSNLSYYTRALPPVADDCPTPMGVKGNKELPDSKEVLEKLLRRRREFIPDPQGS	163
sp   P35354   PGH2_HUMAN	GYKSWEAFSNLSYYTRALPPVDDCPTPLGVKGGKQLPDSNEIVEKLLRRRKFIPDPQGS	180
5F19: A   PDBID   CHAIN   SEQUENCE	GYKSWEAFSNLSYYTRALPPVDDCPTPLGVKGGKQLPDSNEIVEKLLRRRKFIPDPQGS	163
	*****.*****.*****.*****.*****.*****.*****	
6COX: A   PDBID   CHAIN   SEQUENCE	NMMFAFFAQHFTHQFFKTDHKRGPFTRGLGHGVDLNHIYGETLDRQHLRFLKDGKLY	223
sp   P35354   PGH2_HUMAN	NMMFAFFAQHFTHQFFKTDHKRGPFTNGLGHGVDLNHIYGETLARQRKLRFLKDGKMKY	240
5F19: A   PDBID   CHAIN   SEQUENCE	NMMFAFFAQHFTHQFFKTDHKRGPFTNGLGHGVDLNHIYGETLARQRKLRFLKDGKMKY	223
	*****.*****.*****.*****.*****.*****.*****	
6COX: A   PDBID   CHAIN   SEQUENCE	QVIGGEVYPPTVKDTQVEMIYPPHIPENLQFVAGQEVFGLVPLMMYATIWLREHQRVCD	283
sp   P35354   PGH2_HUMAN	QIIDGEMYPPTVKDTQAEMIYPPQVPEHLRFVAGQEVFGLVPLMMYATIWLREHNRVCD	300
5F19: A   PDBID   CHAIN   SEQUENCE	QIIDGEMYPPTVKDTQAEMIYPPQVPEHLRFVAGQEVFGLVPLMMYATIWLREHNRVCD	283
	*. *. *. *****. *****. :. *. *. *****. *****. *****	
6COX: A   PDBID   CHAIN   SEQUENCE	ILKQEHPEWGDEQLFQTSKLILIGETIKIVIEDYVQHLSGYHFCLKFDPPELLFNQGFQYQ	343
sp   P35354   PGH2_HUMAN	VLKQEHPEWGDEQLFQTSRLILIGETIKIVIEDYVQHLSGYHFCLKFDPPELLFNKGFQYQ	360
5F19: A   PDBID   CHAIN   SEQUENCE	VLKQEHPEWGDEQLFQTSRLILIGETIKIVIEDYVQHLSGYHFCLKFDPPELLFNKGFQYQ	343
	. *****. *****. *****. *****. *****. *****	
6COX: A   PDBID   CHAIN   SEQUENCE	NRIASEFNTLYHWHPLLPDTFNIEDQEYSFKQFLYNNISILLEHGLTQFVESFTRQIAGRV	403
sp   P35354   PGH2_HUMAN	NRIAAEFNTLYHWHPLLPDTFQIHDQKYNQQFIYNNISILLEHGITQFVESFTRQIAGRV	420
5F19: A   PDBID   CHAIN   SEQUENCE	NRIAAEFNTLYHWHPLLPDTFQIHDQKYNQQFIYNNISILLEHGITQFVESFTRQIAGRV	403
	***. *****. *. *. *. :. *. *. *****. *****. *****	
6COX: A   PDBID   CHAIN   SEQUENCE	AGGRNVPIAVQAVAKASIDQSRMVKYQSLNEYRKRFLKPYTSFEELTGEKEMAAELKAL	463
sp   P35354   PGH2_HUMAN	AGGRNVPPAVQKVSQASIDQSRMVKYQSFNEYRKRFLKPYESFEELTGEKEMSAELEAL	480
5F19: A   PDBID   CHAIN   SEQUENCE	AGGRNVPPAVQKVSQASIDQSRMVKYQSFNEYRKRFLKPYESFEELTGEKEMSAELEAL	463
	***** ** * . :. *****. *****. ***** ***** *****. *****	
6COX: A   PDBID   CHAIN   SEQUENCE	YSDIDVMELYPALLVEKPRPDAIFGETMVELGAPFSLKGLMGNVICSPQYWKPFSTFGGEV	523
sp   P35354   PGH2_HUMAN	YGDIDAVELYPALLVEKPRPDAIFGETMVEVGAPFSLKGLMGNVICSPAYWKPFSTFGGEV	540
5F19: A   PDBID   CHAIN   SEQUENCE	YGDIDAVELYPALLVEKPRPDAIFGETMVEVGAPFSLKGLMGNVICSPAYWKPFSTFGGEV	523
	*. *. *. :. *****. *****. ***** ***** *****	
6COX: A   PDBID   CHAIN   SEQUENCE	GFKIINTASIQSLICNNVKGCPFTSFNVQDPQPTKATINASASHSRLDDINPTVLIKRR	583
sp   P35354   PGH2_HUMAN	GFQIINTASIQSLICNNVKGCPFTSFVDPPELIKTVINASSSRSLDDINPTVLLKER	600
5F19: A   PDBID   CHAIN   SEQUENCE	GFQIINTASIQSLICNNVKGCPFTSFVSP-----	552
	*. *****. *****. ***** *	
6COX: A   PDBID   CHAIN   SEQUENCE	STEL 587	
sp   P35354   PGH2_HUMAN	STEL 604	
5F19: A   PDBID   CHAIN   SEQUENCE	---- 552	

**Figure S23.** ClustalO<sup>6</sup> multiple alignment between human sequence available in Uniprot P35354, hCOX-2 sequence in 5F19 pdb model<sup>7</sup> and mCOX-2 in 6COX model.<sup>8</sup>

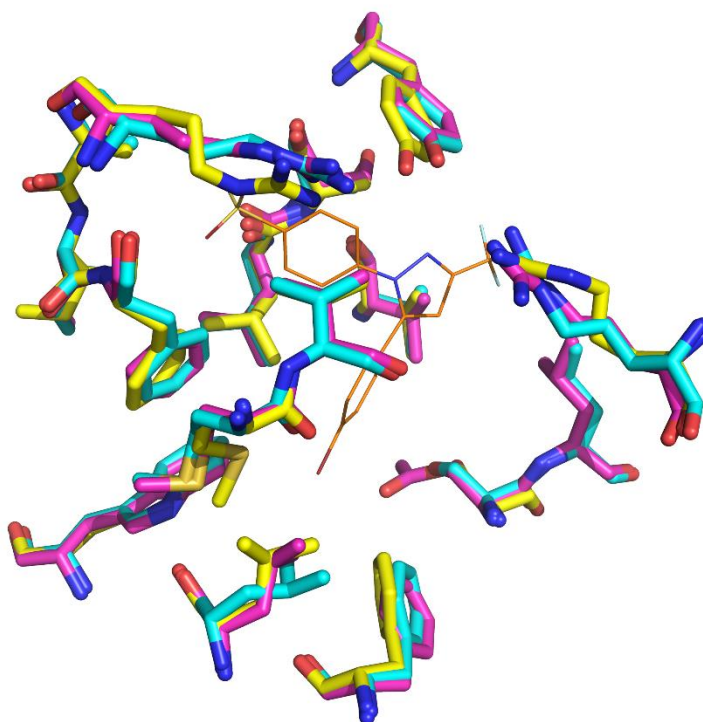


**Figure S24.** Binding site residues alignment of hCOX-2 5F19 (magenta),<sup>7</sup> mCOX-2 6COX (ciano),<sup>8</sup> hCOX-2 theoretical model 1V0X (yellow). SC-558 is represented in orange lines.

**Table S3.** RMSD of aligned structures compared to hCOX-2 5F19.

	Total RMSD	Binding site RMSD
<b>1V0X</b>	0.340	0.273
<b>6COX</b>	0.412	0.4

Since biological test were carried out on human enzymes hCOX 2 the crystal structure with the best resolution was selected for docking studies 5F19.<sup>7</sup>

The coordinates were obtained from the PDB.<sup>1</sup> The protein was prepared with Protein Preparation module available in Maestro GUI.<sup>2</sup> Acetylated Ser530 was mutated in Ser with the “build” tool.

### Docking

Before docking the best compound of the synthesized series (**EMAC10111g**) cross docking experiments were carried out. Four protocols were compared Glide-SP,<sup>9</sup> Glide-XP,<sup>10</sup> Glide Quantum-Mechanical Polarized Docking (QPLD)-SP and QPLD-XP.<sup>11, 12</sup>

In Table S5 are reported the RMSD values between experimental binding mode and first docking pose of each ligand. All protocols can be considered acceptable.

### Ligand preparation

The new ligand **EMAC10111g** was built by means of Maestro GUI<sup>2</sup> in both E/Z configurations. Then a conformational search analysis was performed using MCMC method allowing 5000 iterations in implicit solvent.<sup>3</sup>

Nine conformations were found for “E” configuration and eight for “Z” (Table S4). Previously generated conformers were optimised at DTF level of theory using the B3LYP functional, the 6-31G\*\* basis set and the implicit solvation model PBF water as implemented in Jaguar software.<sup>13</sup>

The molecular mechanics and DFT conformers internal energies were considered for computing the isomers population according to Boltzman analysis at 300 °K. Both set of energy agreed and addressed a population of about 100% to isomer “Z” (Figure S25).

**Table S4.** Conformational search results and population data

Isomer	<i>Molecular mechanics search</i>				<i>DFT optimisation</i>	
	Conformation	Duplicates	<sup>a</sup> Energy	Population%	<sup>a</sup> Energy	Population%
<i>E</i>	1	298	-10.278	0.015	-1407042.844	0.000
	2	314	-10.247	0.015	-1407044.501	0.008
	3	280	-10.243	0.015	-1407041.955	0.000
	4	343	-10.194	0.013	-1407043.253	0.001
	5	321	-10.134	0.012	-1407043.384	0.001
	6	314	-10.108	0.012	-1407042.975	0.001
	7	281	-10.102	0.012	-1407042.301	0.000
	8	545	-10.058	0.011	-1407044.055	0.004
	9	1	-9.743	0.006	-1407044.374	0.006
<i>Overall population</i>				0.110		0.021
<i>Z</i>	1	298	-14.368	14.754	-1407049.518	34.168
	2	275	-14.367	14.741	-1407048.389	5.137
	3	282	-14.367	14.739	-1407049.043	15.401
	4	289	-14.364	14.653	-1407048.247	4.054
	5	282	-14.155	10.331	-1407048.503	6.222
	6	297	-14.152	10.279	-1407049.312	24.192
	7	268	-14.148	10.199	-1407048.417	5.386
	8	290	-14.147	10.194	-1407048.421	5.420
<i>Overall population</i>				99.890		99.979
<sup>a</sup> kcal/mol						

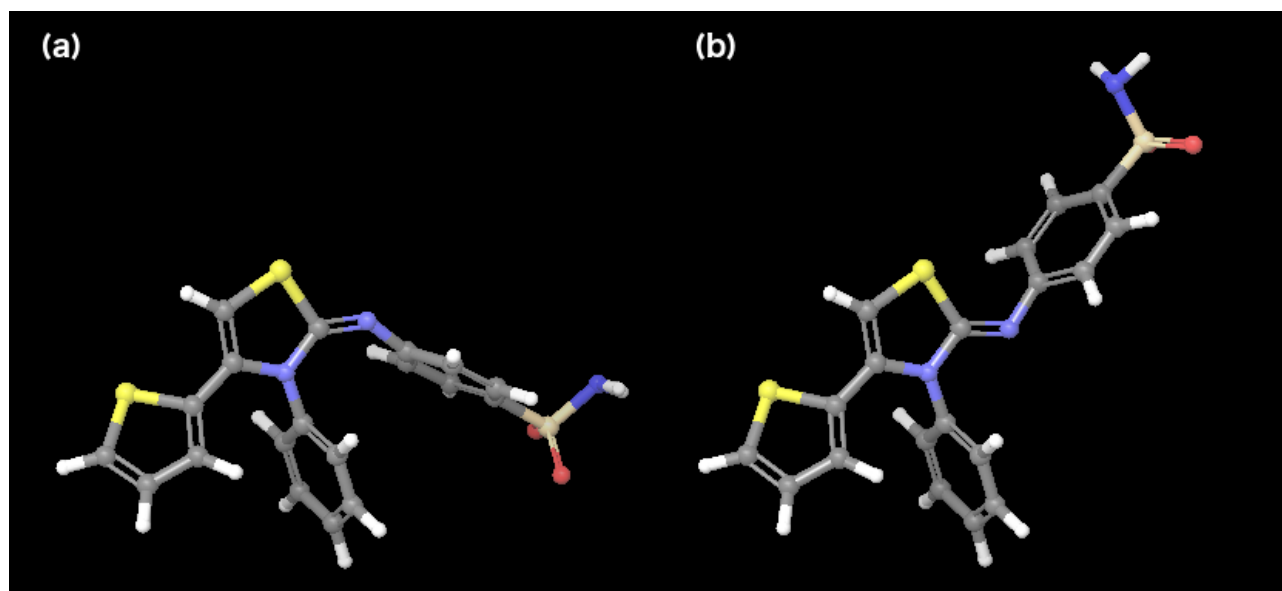


**Figure S25.** (a) (*E*)- and (b) (*Z*)-isomer DFT optimized conformers.

The “Z” configuration was docked applying all protocols. Best pose complex was then minimized to consider the induce fit phenomena and used to analyze the ligand binding mode. 10.000 steps of the Polak-Ribier conjugate gradient (PRCG) minimization method were conducted on the top ranked theoretical

complex using OPLS\_2005 force field.<sup>14</sup> The optimization process was performed up to the derivative convergence criterion equal to  $0.05 \text{ kcal}/(\text{mol} \cdot \text{\AA})^{-1}$ .

### hCOX-1 protein preparation

Since still there are not crystal structures of the hCOX-1 protein available in the Protein Data Bank (PDB), the structure was built with Swiss model, a fully automated protein structure homology-modelling server.<sup>15</sup> The sequence of Prostaglandin G/H synthase 1 protein was retrieved from the Uniprot server (Uniprot code: P23219).

The high sequence identity with the available homologous sheep COX-1 crystal structures (93%) allowed obtaining a reliable model. The quality of the model was assessed by Swiss Model through the measure of QMEAN -0.48 and QMQE 0.89<sup>16</sup> and PROCHECK<sup>17</sup> and through comparison with PDB structure 2AYL<sup>18</sup> which revealed a good alignment of residues in the binding site (Figure S25).

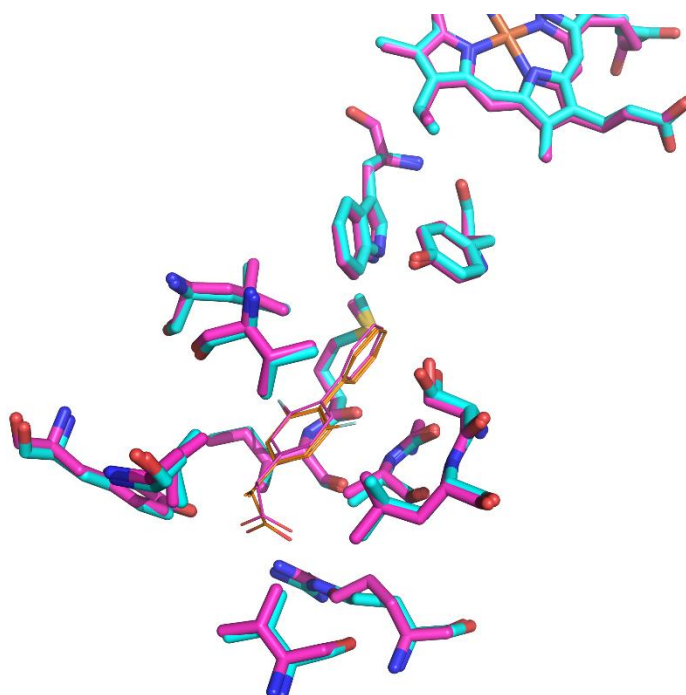


**Figure S25.** Binding site residues alignment of hCOX-1 model (magenta) and oCOX-1 2AYL (cyan). Flurbiprofen is represented in orange lines.

Docking protocol was validated considering the same protocols mentioned above: Glide-SP, Glide-XP, QPLD-SP and QPLD-XP. All protocols can be considered acceptable. Therefore, all were applied to analyze the putative binding mode of new compound. However, it was not possible to dock it into the binding site of hCOX-1 enzyme.

**Table S5.** Cross docking results considering the co-crystallized ligands reported in pdb complexes. All were docked considering hCOX-2 pdb 5F19 and hCOX-1 model.

C O X	PDBID	Compound	hCOX-2				hCOX-1			
			RMSD				RMSD-			
			GlideSP	GlideXP	QPLDSP	QPLDXP	GlideSP	GlideXP	QPLSP	QPLD XP
1	<b>1HT8</b>	Aclofenac	2.79	6.50	//	//	0.58	0.58	//	//
2	<b>1PXX</b>	Diclofenac	1.40		1.38	1.23	0.95		4.51	6.18
1	<b>1Q4G</b>	Biphenylacid	0.90	4.31	0.89	0.86	0.49	0.48	0.48	0.48
1	<b>2AYL</b>	Flurbiprofen	0.90		2.94	0.85	1.00	2.55	2.51	2.55
1	<b>2OYE</b>	Indomethacin-R-Alpha-Ethyl-Ethanolamide	8.16	10.25	2.00	//	//	//	//	//
1	<b>2OYU</b>	Indomethacin-S-Alpha-Ethyl-Ethanolamide	8.56	14.61	//	//	//	11.80	//	//
2	<b>3LN0</b>	5cs	1.17	1.19	1.20	1.14	1.85	1.17	6.00	6.04
2	<b>3LN1</b>	Celecoxib	0.75	1.79	0.74	0.73	//	//	//	//
2	<b>3MQE</b>	Sc75416	7.23	4.03	1.77	4.03	4.09	4.04	6.91	6.82
1	<b>3N8X</b>	Nimesulide	2.03	1.62	1.96	//	2.11	//	//	//
2	<b>3NT1</b>	NaproxenS	0.96	8.43	8.48	1.37	0.53	0.55	0.54	1.13
2	<b>3NTG</b>	23dr	0.72	1.07	0.48	8.44	0.85	0.94	1.05	0.51
2	<b>3Q7D</b>	Naproxen-R	0.95	8.22	8.42	0.62	0.72	0.72	1.34	0.51
2	<b>3QMO</b>	Ns398	0.67	1.81	1.63	//	//	//	//	//
2	<b>3RR3</b>	Flurbiprofen-R	0.58	0.87	0.57	1.38	2.33	0.57	2.77	0.57
2	<b>4COX</b>	Indomethacin	1.52	1.66	1.38	0.57	1.40	1.51	//	1.28
2	<b>4FM5</b>	Desmethylflurbiprofen	2.63	2.42	2.66	0.72	2.31	2.53	2.31	2.53
2	<b>4M10</b>	Isoxicam	6.76	5.98	6.39	//	12.90	6.58	//	//
1	<b>4O1Z</b>	Meloxicam	5.61	5.43	//	//	//	14.02	//	//
2	<b>4OTY</b>	Lumiracoxib	1.27	1.62	3.49	3.76	5.64	3.47	5.59	5.96
2	<b>4PH9</b>	Ibuprofen	0.95	8.29	9.03	//	0.45	1.94	0.45	0.44
2	<b>5IKQ</b>	Meclofenamic acid	0.74	1.06	0.94	0.82	1.11	1.14	1.11	1.11
2	<b>5IKR</b>	Mefenamica acid	0.63	0.97	0.65	0.64	1.15	5.64	1.13	//
2	<b>5IKT</b>	Tolfenamic acid	0.67	0.69	0.73	0.60	1.49	1.28	1.46	1.25
2	<b>5IKV</b>	Flufenamic acid	0.62	0.72	2.18	1.90	2.08	//	1.02	2.09
2	<b>5KIR</b>	Rofecoxib	1.66	1.07	8.04	1.69	//	//	//	//
1	<b>5U6X</b>	P6	7.34	6.12	7.14	7.30	8.01	7.19	8.45	
2	<b>5W58</b>	Arn2508	10.87	10.74	11.00	10.87	10.95	10.95	10.95	10.75
1	<b>5WBE</b>	Mofezolac	0.75	6.90	6.27	7.29	0.99	0.99	//	0.99
2	<b>6COX</b>	Sc558	0.67	1.63	0.62	0.61	//	//	//	//

### Docking experiments on Human Carbonic Anhydrase XII, IX and II

Docking experiments were performed by means of the previously validated protocol<sup>19</sup> Glide QPLD-XP. The ligands sulfonamide group was considered in the deprotonated anionic form. We performed also for this

enzymes a cross docking experiment including the experimental binding mode information of new uploaded complexes. For hCA II, due to the high number of crystal structures, we randomly selected 15 pdb structures with high resolution.

**Table S6.** Cross docking results considering the co-crystallized ligands reported in pdb complexes. Receptor coordinates were obtained considering hCAX II pdb 4WW8<sup>20</sup> and hCA IX pdb 4FL4<sup>21</sup> and hCA IX pdb 3K34.<sup>22</sup>

hCAX II			hCA IX			hCA II		
PDB	PDB RES. (Å)	RMSD	PDB	PDB RES (Å)	RMSD	PDB	PDB RES. (Å)	RMSD
1JD0	1.5	1.33	3IAI	2.2	2.00	3B4F	1.89	2.27
4HT2	1.45	1.89	5FL4	1.82	1.73	3K34	0.9	2.59
4KP5	1.45	3.36	5FL5	2.05	2.28	3M67	1.8	4.19
4KP8	1.8	2.82	5FL6	1.95	2.25	3N3J	1.5	2.02
4Q0L	2	3.06	6FE0	1.91	1.12	3PO6	1.47	2.14
4QJ0	1.55	1.18	6FE1	1.95	1.03	3R16	1.6	3.21
4QJO	1.8	1.91	6G9U	1.75	10.11	3S9T	1.3	2.95
4QJW	1.55	2.33	6G98	2.47	8.43	3SBH	1.65	3.53
4WW8	1.42	0.89				4ITO	1.16	4.22
5LL5	1.42	4.33				4IWZ	1.59	3.16
5LL9	1.45	3.38				4K13	1.6	2.48
5LLO	1.6	2.11				5FDI	1.85	4.24
5LLP	1.48	2.45				5LL4	1.12	3.00
5MSA	1.2	1.60				5TFX	1.5	2.63
5MSB	1.3	1.75				6B4D	1.19	2.38

This protocol was then applied to dock the (Z)-EMAC10111g. The best complexes were then minimized as described for hCOX-2 complex.

Depictions were taken by means of Pymol<sup>23</sup> and Maestro GUI.<sup>2</sup>



## Biological evaluation

### Carbonic anhydrase inhibition assay

The purification of cytosolic CA isoenzymes (CA I and CA II) were previously described with a simple one-step method by a Sepharose-4B-L tyrosine-sulphanilamide affinity chromatography <sup>24</sup>. The protein quantity in the column effluents was determined spectrophotometrically at 280 nm. Sodium dodecyl sulphate-polyacrylamide gel electrophoresis (SDS-PAGE) was applied with a Bio-Rad Mini Gel system Mini-PROTEIN<sup>®</sup> system, Bio-Rad Laboratories, Inc., China after purification of both CA isoenzymes. Briefly, it was performed in acrylamide for the running (10%) and the stacking gel (3%) contained SDS (0.1%), respectively. Activities of CA isoenzymes were determined according to a method by Verporte et al.<sup>25</sup> The increase in absorbance of reaction medium was spectrophotometrically recorded at 348 nm. Also, the quantity of protein was determined at 595 nm according to the Bradford method <sup>26</sup>. Bovine serum albumin was used as standard protein. The IC<sub>50</sub> values were obtained from activity (%) versus compounds plots <sup>27</sup>. For calculation of K<sub>I</sub> values, three different concentrations were used. The Lineweaver–Burk curves were drawn and calculations were realised <sup>27</sup>.

### Determination of human cyclooxygenase isoform activity

The biological evaluation of the test drugs on total hCOX activity (bisdioxygenase and peroxidase reactions) was investigated by measuring their effects on the oxidation of N,N,N',N'-tetramethyl-p-phenylenediamine (TMPD) to N,N,N',N'-tetramethyl-p-phenylenediimine, using arachidonic acid as common substrate for both hCOX-1 and hCOX-2, microsomal COX-2 prepared from insect cells (Sf 21 cells) infected with recombinant baculovirus containing cDNA inserts for hCOX-2 (Sigma–Aldrich Química S.A., Alcobendas, Spain) and COX-1 from human platelet microsomes obtained as previously reported by some of us <sup>28</sup>. The formation of N,N,N',N'-tetramethyl-p-phenylenediimine (a coloured compound) from N,N,N',N'-tetramethyl-p-phenylenediamine catalysed by COX can be detected spectrophotometrically at 600 nm. In this study, hCOX activity was evaluated using the above spectrophotometric method slightly modifying the procedure reported by Copeland and co-workers <sup>29</sup>. Briefly, 0.1 mL of Tris–HCl buffer (100 mM, pH 8) containing 1 mM hematin, 100 mM TMPD, various concentrations of the test drugs (new compounds or reference inhibitors), and appropriate amounts of hCOX-1 and hCOX-2 required and adjusted to obtain under our experimental conditions the same control absorbance increase (0.08 A<sub>600</sub> U/min) were incubated for short periods of time (3–5 min) to avoid a notable loss of COX activity at 37°C in a flat-bottom 96-well microtest plate (BD Biosciences, Franklin Lakes, NJ, USA) placed in the dark multimode microplate reader chamber. After this incubation period, the reaction was started by adding (final concentration) 100 mM arachidonic acid and the formation of N,N,N',N'-tetramethyl-p-phenylenediimine from TMPD, i.e., the increase in absorbance at 600 nm was measured at 37°C in a multi-mode microplate reader (Fluostar Optima, BMG Labtech GmbH, Offenburg, Germany) for 25 s, a period in which the absorbance increased linearly from the beginning. The specific absorbance (used to obtain the final results) was calculated after subtraction of the background absorbance generated in wells containing a blank solution, i.e., all components except the COX isoforms, which were replaced by a Tris–HCl buffer solution. Under our experimental conditions, this background activity was practically negligible. Control experiments were carried out simultaneously by replacing the test drugs (new compounds and reference inhibitors) with appropriate dilutions of the vehicles. In addition, the possible capacity of the above test drugs to modify the absorbance of the reaction mixture due to non-enzymatic inhibition (e.g., for directly reacting with TMPD) was determined by adding these drugs to solutions containing only TMPD in a Tris–HCl buffer solution.

## References

1. Berman, H. M.; Westbrook, J.; Feng, Z.; Gilliland, G.; Bhat, T. N.; Weissig, H.; Shindyalov, I. N.; Bourne, P. E., The protein data bank. *Nucleic Acids Research* **2000**, *28* (1), 235-242.
2. Schrödinger LLC.: New York, N., USA, 2018.
3. Mohamadi, F.; Richards, N. G.; Guida, W. C.; Liskamp, R.; Lipton, M.; Caufield, C.; Chang, G.; Hendrickson, T.; Still, W. C., MacroModel—an integrated software system for modeling organic and bioorganic molecules using molecular mechanics. *Journal of Computational Chemistry* **1990**, *11* (4), 440-467.
4. Halgren, T. A., Merck molecular force field. II. MMFF94 van der Waals and electrostatic parameters for intermolecular interactions. *Journal of Computational Chemistry* **1996**, *17* (5-6), 520-552.
5. Kollman, P. A.; Massova, I.; Reyes, C.; Kuhn, B.; Huo, S.; Chong, L.; Lee, M.; Lee, T.; Duan, Y.; Wang, W.; Donini, O.; Cieplak, P.; Srinivasan, J.; Case, D. A.; Cheatham, T. E., Calculating structures and free energies of complex molecules: combining molecular mechanics and continuum models. *Accounts of Chemical Research* **2000**, *33* (12), 889-897.
6. Sievers, F.; Higgins, D. G., Clustal Omega for making accurate alignments of many protein sequences. *Protein science : a publication of the Protein Society* **2018**, *27* (1), 135-145.
7. Lucido, M. J.; Orlando, B. J.; Vecchio, A. J.; Malkowski, M. G., Crystal Structure of Aspirin-Acetylated Human Cyclooxygenase-2: Insight into the Formation of Products with Reversed Stereochemistry. *Biochemistry* **2016**, *55* (8), 1226-1238.
8. Kurumbail, R. G.; Stevens, A. M.; Gierse, J. K.; McDonald, J. J.; Stegeman, R. A.; Pak, J. Y.; Gildehaus, D.; iyashiro, J. M.; Penning, T. D.; Seibert, K.; Isakson, P. C.; Stallings, W. C., Structural basis for selective inhibition of cyclooxygenase-2 by anti-inflammatory agents. *Nature* **1996**, *384*, 644.
9. Friesner, R. A.; Banks, J. L.; Murphy, R. B.; Halgren, T. A.; Klicic, J. J.; Mainz, D. T.; Repasky, M. P.; Knoll, E. H.; Shelley, M.; Perry, J. K.; Shaw, D. E.; Francis, P.; Shenkin, P. S., Glide: A New Approach for Rapid, Accurate Docking and Scoring. 1. Method and Assessment of Docking Accuracy. *Journal of Medicinal Chemistry* **2004**, *47* (7), 1739-1749.
10. Abdel Hafez, O. M.; Amin, K. M.; Abdel-Latif, N. A.; Mohamed, T. K.; Ahmed, E. Y.; Maher, T., Synthesis and antitumor activity of some new xanthotoxin derivatives. *European journal of medicinal chemistry* **2009**, *44* (7), 2967-74.
11. Cho, A. E.; Guallar, V.; Berne, B. J.; Friesner, R., Importance of accurate charges in molecular docking: quantum mechanical/molecular mechanical (QM/MM) approach. *J Comput Chem* **2005**, *26* (9), 915-31.
12. Chung, J. Y.; Hah, J. M.; Cho, A. E., Correlation between performance of QM/MM docking and simple classification of binding sites. *Journal of chemical information and modeling* **2009**, *49* (10), 2382-7.
13. *Jaguar, version 9.0, Schrödinger, LLC, New York, NY, 2015.*
14. Jorgensen, W. L., OPLS force fields. *Encyclopedia of computational chemistry* **1998**.
15. Arnold, K.; Bordoli, L.; Kopp, J.; Schwede, T., The SWISS-MODEL workspace: a web-based environment for protein structure homology modelling. *Bioinformatics (Oxford, England)* **2006**, *22* (2), 195-201.
16. Benkert, P.; Tosatto, S. C.; Schomburg, D., QMEAN: A comprehensive scoring function for model quality assessment. *Proteins* **2008**, *71* (1), 261-77.
17. Morris, A. L.; MacArthur, M. W.; Hutchinson, E. G.; Thornton, J. M., Stereochemical quality of protein structure coordinates. *Proteins* **1992**, *12* (4), 345-64.
18. Gupta, K.; Selinsky, B. S.; Loll, P. J., 2.0 A structure of prostaglandin H2 synthase-1 reconstituted with a manganese porphyrin cofactor. *Acta Crystallographica Section D* **2006**, *62* (2), 151-156.
19. Bianco, G.; Meleddu, R.; Distinto, S.; Cottiglia, F.; Gaspari, M.; Melis, C.; Corona, A.; Angius, R.; Angeli, A.; Taverna, D.; Alcaro, S.; Leitans, J.; Kazaks, A.; Tars, K.; Supuran, C. T.; Maccioni, E., N-Acylbenzenesulfonamide dihydro-1,3,4-oxadiazole hybrids: seeking selectivity toward carbonic anhydrase isoforms. *ACS Medicinal Chemistry Letters* **2017**, *8* (8), 792-796.
20. Zubriene, A.; Smirnoviene, J.; Smirnov, A.; Morkunaite, V.; Michailoviene, V.; Jachno, J.; Juozapaitiene, V.; Norvaisas, P.; Manakova, E.; Grazulis, S.; Matulis, D., Intrinsic thermodynamics of 4-substituted-2,3,5,6-tetrafluorobenzenesulfonamide binding to carbonic anhydrases by isothermal titration calorimetry. *Biophysical chemistry* **2015**, *205*, 51-65.

21. Leitans, J.; Kazaks, A.; Balode, A.; Ivanova, J.; Zalubovskis, R.; Supuran, C. T.; Tars, K., Efficient Expression and Crystallization System of Cancer-Associated Carbonic Anhydrase Isoform IX. *Journal of Medicinal Chemistry* **2015**, *58* (22), 9004-9009.
22. Behnke, C. A.; Le Trong, I.; Godden, J. W.; Merritt, E. A.; Teller, D. C.; Bajorath, J.; Stenkamp, R. E., Atomic resolution studies of carbonic anhydrase II. *Acta crystallographica. Section D, Biological crystallography* **2010**, *66* (Pt 5), 616-27.
23. The PyMOL Molecular Graphics System Version 1.7 Schrödinger, L. L. C.
24. Akbaba, Y.; Akincioglu, A.; Gocer, H.; Goksu, S.; Gulcin, I.; Supuran, C. T., Carbonic anhydrase inhibitory properties of novel sulfonamide derivatives of aminoindanes and aminotetralins. *J. Enzyme Inhib. Med. Chem.* **2014**, *29* (1), 35-42.
25. Verpoorte, J. A.; Mehta, S.; Edsall, J. T., Esterase activities of human carbonic anhydrases B and C. *J. Biol. Chem.* **1967**, *242* (18), 4221-9.
26. Bradford, M. M., A rapid and sensitive method for the quantitation of microgram quantities of protein utilizing the principle of protein-dye binding. *Anal. Biochem.* **1976**, *72* (1-2), 248-54.
27. Senturk, M.; Gulcin, I.; Beydemir, S.; Kufrevioglu, O. I.; Supuran, C. T., In vitro inhibition of human carbonic anhydrase I and II isozymes with natural phenolic compounds. *Chem. Biol. Drug Des.* **2011**, *77* (6), 494-499.
28. Carradori, S.; Secci, D.; Bolasco, A.; De Monte, C.; Yáñez, M., Synthesis and Selective Inhibitory Activity Against Human COX-1 of Novel 1-(4-Substituted-thiazol-2-yl)-3,5-di(hetero)aryl-pyrazoline Derivatives. *Archiv der Pharmazie* **2012**, *345* (12), 973-979.
29. Copeland, R. A.; Williams, J. M.; Giannaras, J.; Nurnberg, S.; Covington, M.; Pinto, D.; Pick, S.; Trzaskos, J. M., Mechanism of selective inhibition of the inducible isoform of prostaglandin G/H synthase. *Proc. Natl. Acad. Sci. U. S. A.* **1994**, *91* (23), 11202.